Combined water table and temperature dynamics control CO_2 emission estimates from drained peatlands under rewetting and climate change scenarios

Tanja Denager[1], Jesper Riis Christiansen[2], Raphael Johannes Maria Schneider[1], Peter Langen[3], Thea Quistgaard[3], Simon Stisen[1]

[1] Department of Hydrology, Geological Survey of Denmark and Greenland, Copenhagen, Denmark
[2] Forest and Landscape Ecology, Department of Geoscience and Nature Management, Copenhagen University, Denmark
[3] Department of Environmental Science, Atmospheric Emissions & Modelling, Aarhus University, Roskilde, Denmark

Correspondence to: Tanja Denager (tad@geus.dk)

Abstract:

This study integrates process-based hydrological modeling and empirical CO_2 flux modeling at a daily temporal resolution to evaluate how peatland hydrology influence CO_2 emissions under scenarios of rewetting and climate change.

Following the calibration of a three-dimensional transient groundwater flow model for a peat-dominated catchment, daily groundwater table dynamics were simulated to represent hydrological conditions in drained peat soils. These simulations were coupled with an empirical CO_2 flux model, developed from a comprehensive daily dataset of groundwater table depth, temperature, and soil CO_2 flux measurements. The empirical CO_2 flux model captures a clear temperature-dependent response of soil CO_2 emissions to variations in groundwater table depth.

By applying this coupled modeling framework, we quantified CO_2 emissions at daily timescales. The results demonstrate that incorporating both temperature sensitivity and high-resolution temporal variability in water level significantly influences projections of CO_2 fluxes. Especially the co-occurrence of elevated air temperature and low groundwater table significantly influence CO_2 emissions under scenarios of rewetting and climate change. These insights highlight the importance of including changing climate conditions in future peatland management strategies for emission inventories.

The study illustrates the value of combining detailed hydrological simulations with emission models. It also emphasizes the need for detailed monitoring of greenhouse gas emissions across multiple sites and the development of robust empirical models that can be generalized and spatially upscaled.

Introduction

Drained peatlands are widely accepted as being net greenhouse gas (GHG) sources and rewetting of peatlands is considered an effective means of overall net GHG emission reduction (Leifeld et al., 2019). The depth of the groundwater table below the surface i.e. the water table depth (WTD) largely controls the annual emissions of carbon dioxide (CO_2) and methane (CH_4) from organic soils, where deeper WTD results in CO_2 emissions and a shallow WTD increases CH_4 emissions (Evans et al., 2021). Despite triggering CH_4 emissions, rewetting of organic soils will still lead to a net long-term reduction of GHG emissions (Günther et al., 2020). However, current estimates of GHG emissions from drained and rewetted peatlands are still quite uncertain due to a lack of long-term monitoring and simplified modeling approaches.

Commonly adopted methodologies for estimating contribution of organic soils in national GHG inventories (Arents et al., 2018; Evans et al., 2021; Koch et al., 2023; Tiemeyer et al., 2020) are based on empirical response functions between long-term annual mean WTD estimates from data-driven machine learning (ML) models (Bechtold et al., 2014; Koch et al., 2023) and observed net ecosystem GHG budgets (Tiemeyer et al. 2020). Those methodologies allow regional upscaling and integration into national emission estimates.

However, significant variability in the observed net ecosystem carbon balance (NECB) used to derive the empirical relationship can be attributed to site-specific factors, including intra-annual (seasonal) WTD and temperature dynamics (Tiemeyer et al., 2020) caused by fluctuating climate. The current GHG inventory methods are not suited to account for extremes such as drought and flooding that have a profound, but temporally limited (days, weeks or months) impact on WTD. Especially the frequency and severity of droughts can have major impacts on the CO_2 emissions as WTD increases together with temperature (Olefeldt et al., 2017). Therefore, temperature changes also directly impact GHG emissions, as soil CO_2 and CH_4 production are temperature sensitive. Currently, the impact of short-term compound events (e.g., simultaneous warm and dry conditions (Zscheischler et al., 2020) on annual CO_2 emissions from peat soil is little known. Such events can lead to consequences like a deep groundwater table, highlighting the need for improved understanding of how climate variability and long-term change (Olefeldt et al., 2017) affect future CO_2 emissions from both drained and rewetted peatlands.

For Denmark, it is generally expected that, as a result of climatic changes, annual mean WTD will decrease (water tables closer to surface). However, this decrease in annual mean WTD is primarily attributed to a decrease in WTD during the wetter winter months, while warmer future summers are anticipated to experience minimal decrease or even increase in summer WTD (water tables deeper below the surface) and more prolonged periods with increased WTD (Henriksen et al., 2023; Seidenfaden et al., 2022).

The ML and statistical models of annual mean WTD (Bechtold et al., 2014; Koch et al., 2023) utilized in current national GHG inventories (Gyldenkærne et al., 2025; Koch et al., 2023; Nielsen et al., 2025b; Tiemeyer et al., 2020) effectively reflect the spatial variability at the national scale, but most current ML WTD models are temporally invariant and account for neither inter-annual (between-year) variability nor seasonal or intra-annual variability in WTD or temperature. . To establish WTD-CO_2 relations at intra-annual time scales, capable of capturing the impact of short-lived extreme events such as droughts and inundations, WTD time series at these finer temporal resolutions are required. For this, process-based transient 3D hydrological models capable of integrating unsaturated-saturated flow models to predict spatial and temporal variability of WTD are highly useful. Combined with the WTD-CO_2 relation we claim these model outputs can be used to calculate the CO_2 emissions on daily, seasonal, and inter-annual timescales.

Such hydrological models provide the potential for improving our estimation of peatland hydrology and thereby the spatio-temporal WTD variability. Improved representation of temporal variability of WTD are needed for refining the current and future GHG estimates that cannot be derived using the simple application of IPCC default emission factors (IPCC, 2014). Process-based hydrological models offer the opportunity to assess the effect of different management strategies and environmental conditions, such as rewetting and climate change.

Process-based hydrological models are increasingly being applied to study dynamics of peatland hydrology (Mozafari et al., 2023). For instance, Land Surface Models (LSM) (Bechtold et al., 2019; Largeron et al., 2018; Shi et al., 2015; Yuan et al., 2021) are employed to analyze the soil–plant–atmosphere exchange processes of water, energy and carbon. However, most LSM's rely on a simplified conceptual representation of hydrologic processes and are characterized by coarse spatial scales.

Of the studies applying fully integrated unsaturated-saturated flow models for peatland hydrology, some focus on site or field-scale models (Friedrich et al., 2023; Haahti et al., 2015; Java et al., 2021; Stenberg et al., 2018) while others apply the models at catchment scale (Ala-aho et al., 2017; Duranel et al., 2021; Friedrich et al., 2023; Jutebring et al., 2018; Lewis et al., 2013). A catchment scale approach with water balance closure is particularly important for climate change impact predictions, since the boundary conditions to the peatlands will also be affected by climate change. Similarly, the use of catchment scale models is important because impact evaluations of peatland management scenarios, such as rewetting, can also include impacts on streamflow and groundwater levels in neighboring areas.

The objectives of this study were to 1) estimate current and predict the future hydrology and soil CO_2 emissions in a Northern European drained peatland and 2) investigate the role of rewetting and climatic extremes on annual CO_2 emissions. To achieve these objectives, we used a transient physically-based hydrological 3D model to predict daily WTD for a case study area, the Tuse Stream catchment, representing a typical degraded Danish peatland. Secondly, we developed an empirical soil CO_2 flux (fCO_2) model based on coupled CO_2 flux, WTD and temperature observations for a similar Danish peatland (Nielsen et al., 2025a), capable of making daily predictions. Combining the mechanistic hydrological model and the empirical emission model enabled the estimation of daily soil CO_2 fluxes under current conditions as well as scenarios of rewetting and future climate, while accounting for the impact of climatic variability and extremes.

Data and methodology

Study area

Tuse Stream catchment is located on the island of Zealand in the eastern part of Denmark (Figure 1a). The total area encompasses 107 km^2 of which 19 km^2 are peat soil. The areal extent of peat soil was determined using a national map of organic soils (Adhikari et al., 2014). The largest continuous peat area within the catchment is a 13 km^2 drained fen located in a river valley (Figure 1c) in the low-lying part of the catchment. The peat soil area is primarily used for agriculture. In small parts of the area, the drainage has been stopped to restore the natural hydrologic regime. The measured peat layer thickness extends from 0.4 to 3.5 meters, below which alluvial sand deposits are typically found. Generally, the deeper geology in the area can be characterized as clay-dominated glacial till deposits. The catchment is characterized by flat topography, with the southern part of the catchment being hillier. The climate conditions are humid and temperate. The catchment receives about 737 mm of precipitation per year (1990-2024) and has an annual mean temperature of 9°C (Scharling, 1999a, b).

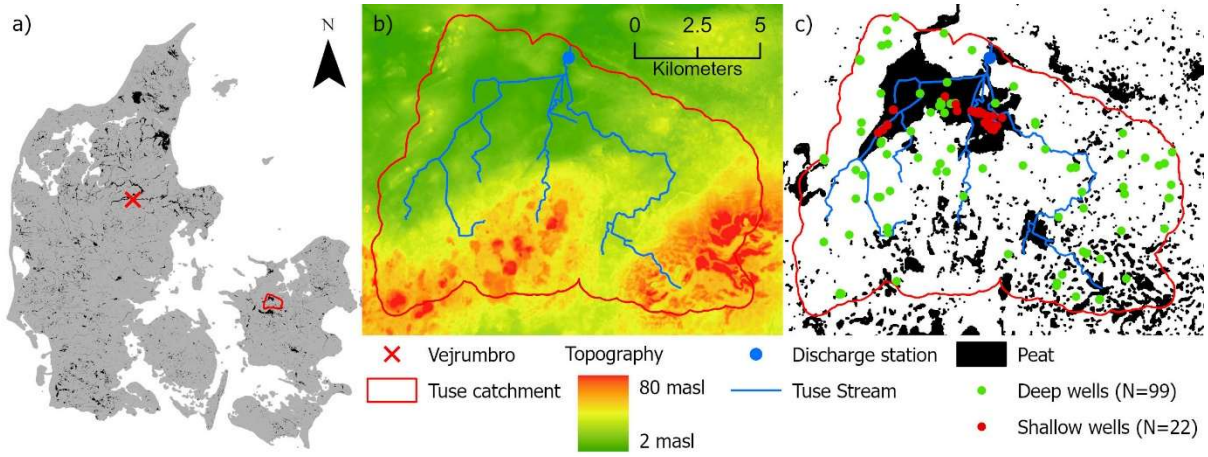

Figure 1: a) Location of Tuse Stream catchment and the Vejrumbro site, b) topography and stream network of Tuse Stream catchment, masl: meter above sea level, c) location of organic soil and observation wells in the Tuse Stream catchment.

Shallow WTD in the drained organic soils is monitored in 22 groundwater wells (2-3.5 meters deep) (Figure 1c). The wells are fully screened and WTD is automatically logged with pressure transducers at an hourly basis (aggregated to daily values) and verified with manual measurements. All WTD data are available in the Danish National Well Database (Jupiter, 2025). In this study, we define the water table depth (WTD) as positive when located below the surface and negative when above the surface. Monitoring data includes additional point measurements and timeseries of groundwater head from 99 deep wells installed in mineral soils throughout the catchment (Figure 1c). In the model setup, water extraction in 40 abstraction wells is included based on data from the Danish National Well Database in May 2020 (Henriksen et al., 2020) and implemented as yearly mean abstraction evenly distributed on the daily model timesteps. Daily discharge is monitored at the catchment outlet at Tuse Stream (Figure 1b).

Hydrological modelling

The focus of the hydrological modelling in this study is to adequately simulate shallow groundwater levels and their dynamics for the peatland area in the Tuse Stream catchment. The fen peatland in Tuse Stream catchment is largely fed by groundwater discharge from the upstream catchment, emphasizing the need to develop a coupled groundwater surface water model at catchment scale. In addition, the objective of utilizing the model for climate change impact assessments requires a catchment scale approach with a deep groundwater component to represent changes in groundwater and surface water discharge to the peatland as well as changes in the boundary conditions. The catchment scale approach also facilitates the combined calibration and evaluation of the total water balance and peatland WTD by constraining the model with observed streamflow at the outlet as well as peatland groundwater level dynamics.

The model is set up as a transient, distributed, coupled surface-groundwater model and executed within the hydrological modeling framework MIKE SHE (DHI, 2022; Graham and Butts, 2005). MIKE SHE combines full 3D groundwater flow coupled with a gravity flow module in the unsaturated zone, 2D overland flow and 1D river flow routing in streams (DHI, 2019) (Figure S1). The simplified gravity flow module for unsaturated flow assumes a uniform vertical gradient and ignores capillary forces but provides a suitable solution for the time varying recharge to the groundwater table based on precipitation and evapotranspiration (DHI, 2022).

The model is a modified sub-model of the National Hydrological Model of Denmark (DK-model), developed at the Geological Survey of Denmark and Greenland (GEUS) (Henriksen et al., 2020; Stisen et al., 2019). The geological model is interpreted in a horizontal 100 meter grid. The numerical model is

calibrated in the same 100 meter resolution, with the saturated zone consisting of 11 computational layers of varying thickness. The top model layer has a uniform thickness of 2 meters, which is also applied to the peat layer areas. The bottom level of the groundwater model is defined by the prequaternary chalk that underlies the Island of Zealand, which in the Tuse Stream catchment is located in a depth of approximately 150-250 meters below surface.

The time-varying constant head boundary conditions at the sub-model boundary are defined from the operational National Hydrological Model setup (Henriksen et al., 2020). The observed forcing data of precipitation, temperature and reference evapotranspiration are provided by the Danish Meteorological Institute (DMI) as gridded daily data in 10 km resolution for precipitation and 20 km resolution for evapotranspiration and temperature (Scharling, 1999a, b; Stisen et al., 2011). The model employs a maximum timestep of one day, at which the meteorological variables are fed into the model. The model was provided with a hotstart file from an initial model run.

Spatial and temporal distributions of root depth and LAI are based on classes (Figure S2 and Table S1) where the peat, forest, agricultural and open nature land use classes have yearly cycles of LAI and root depth (Figure S3). Likewise, soil type is spatially distributed (Figure S2) and based on the three classes peat, sand and clay (Table S2). In the vertical direction, the soil columns in the unsaturated zone module are divided into 40 cells from top to bottom; 30x0.1m, 5x1m and 5x5m. Technically, the unsaturated zone is parameterized to 33 m depth, but during simulation limited to the top of the simulated groundwater table. We implemented uniform vertical water retention characteristics of peat, while clay and sand water retention characteristics were defined separately for the depths 0-30 cm (horizon A), 30-70 cm (horizon B) and >70 cm (horizon C). Soil parameterization is freely adapted from (Børgesen et al., 2009) and detailed in Table S3.

MIKE SHE allows incorporation of drainage systems, representing both artificial and natural drains. The drainage system bypasses the slow water movement in aquifers by providing a short-cut from e.g. the agricultural field to the nearest stream. The amount of water routed by drains from the saturated zone to local surface water bodies is calculated using a linear reservoir model, where the difference between groundwater head and drain level is multiplied by a drain time constant (*dt*). The drain level is defined by a drain depth (*dd*) set relative to surface level. Hence, drainage in any given model cell only occurs if the simulated groundwater level exceeds the drainage level (DHI, 2022). The drain time constant and drainage depth in each model grid cell are distributed across the model domain according to the five land use classes (Figure S2 and Table S1).

The model parameter sensitivity analysis and subsequent calibration prioritized parameters affecting the shallow WTD in the peat soil and the overall water balance in the catchment. A list of model parameters can be seen in Table S3. Parameter values not included in the calibration process are obtained from the National Hydrological Model parametrization.

Calibration method

We used the Pareto Archived Dynamically Dimensioned Search (PADDS) algorithm (Asadzadeh and Tolson, 2013) available within the optimization toolkit Ostrich (Matott, 2019). PADDS is a multi-objective optimizer and obtains the pareto front across multiple objective function groups, enabling post-weighting of individual objective functions. Throughout the calibration routine, Ostrich minimized the weighted sum of squared error (WSSE) of each of the objective function groups. The PADDS algorithm was run with the user settings of maximum 1000 iterations. The period 2010-2013 was used as a calibration spin-up period and the model performance was evaluated for the 2014-2023 calibration period.

Calibration was performed against three objective function groups: $KGE_{WTD\_modified}$, $r_{spatial}$ and $KGE_qME_{head}ME_{amp}$. The $KGE_{WTD\_modified}$ objective group is used to optimize the model performance with respect to the WTD in peatlands. KGE is the Kling-Gupta Efficiency and consists of three terms: the Pearson correlation coefficient r, a term representing the measure of variability α and a bias term β. In KGE, β is a unitless measure of the bias specified as the ratio between the sum of simulated and observed values ($\beta = \sum sim/\sum obs$). As we use KGE to optimize the WTD (and not hydraulic head), the operational sign can be both negative (water table above surface/inundation) and positive (water table below surface), violating the idea of optimizing β as the ratio of sums of values with possibly alternating operational signs. Therefore, we are using $KGE_{WTD\_modified}$ where β is replaced by the mean error (ME) (Table 1). This modification requires that the order of magnitude of the ME_{WTD} is comparable to the errors on the other terms in KGE. In our case this is ensured by the fact that the mean observed WTD values range between approximately 0.3-0.6 m, resulting in ME_{WTD} values typically below 0.5 m. Alternatively, the ME_{WTD} term could be scaled within the KGE_{WTD} equation.

The calibration using the $KGE_{WTD\_modified}$ as objective function group aims at achieving the best overall agreement between simulated and observed WTD. However, during first calibration experiments, we found that this objective function group primarily focuses on the temporal dynamics of WTD. To improve the representation of the spatial variability of the mean WTD, the correlation coefficient ($r_{spatial}$) was included as an additional objective function group (Table 1).

$KGE_qME_{head}ME_{amp}$ is an objective function group that combines three performance criteria: the Kling-Gupta Efficiency performance criterion for discharge (KGE_q), the mean error of hydraulic head in deeper aquifers (ME_{head}) and the mean error of annual amplitude of hydraulic head in the deeper aquifers (ME_{amp}). For a detailed description of the implementation of ME_{amp} as objective function see (Henriksen et al., 2020). This objective function group was included to optimize the overall water balance and streamflow dynamics expressed through the discharge at the catchment outlet (KGE_q), to match the general water level in the deeper aquifers across the catchment (ME_{head}), and to match the natural seasonal variations in hydraulic head (ME_{amp}). As the metrics of KGE_q, ME_{head} and ME_{amp} are combined into one objective function group, we need to weigh the observations, to ensure that KGE_q, ME_{head} and ME_{amp} affect the objective group of $KGE_qME_{head}ME_{amp}$ approximately equally. This was done based on WSSE from a model run with initial parameter values.

Table 1: Objective functions metrics. KGE stands for Kling-Gupta Efficiency.

Objective function group	Observations	No. of observation wells	Metric	Abbreviation	Equation	Range	Optimum value
$KGE_{WTD\_modified}$	Daily WTD in shallow wells (in peat)	22	Modified KGE on WTD	$KGE_{WTD\_modified}$	$1-\sqrt{(r_{WTD}-1)^2+(\alpha_{WTD}-1)^2+(ME_{WTD})^2}$ Where, $ME_{WTD}=\frac{1}{n}\sum_{i=1}^{n} WTD_{sim_i}-WTD_{obs_i}$	[-∞;1]	1
$r_{spatial}$	Mean WTD over the calibration period	22	Spatial correlation of the mean WTD	$r_{spatial}$	$r(\overline{WTD_{sim}},\overline{WTD_{obs}})$	[-1;1]	1
$KGE_q ME_{head} ME_{amp}$	Discharge	1	KGE on discharge	KGE_q	$1-\sqrt{(r_q-1)^2+(\alpha_q-1)^2+(\beta_q-1)^2}$	[-∞;1]	1
	Hydraulic head in deep wells (in mineral soil)	66	Mean error on hydraulic heads	ME_{head}	$\frac{1}{n}\sum_{i=1}^{n} head_{sim_i}-head_{obs_i}$	[-∞;∞]	0
		8	Mean error on yearly amplitude of hydraulic heads	ME_{amp}	$\frac{1}{n}\sum_{i=1}^{n} A_{sim_i}-A_{obs_i}$	[-∞;∞]	0

WTD: water table depth [m], q: discharge [m/s], head: hydraulic head [m], A: amplitude [m]

A local sensitivity analysis based on initial parameter values from Table S4 was performed and values of composite scaled sensitivity (CSS) were obtained. Selection of free calibration parameters were based on the criterion that parameters were included if their CSS was larger than 0.05*CSS of the parameter with the highest CSS. The resulting 11 free parameters are indicated with grey in Table S4. Other parameters were kept at the values listed in Table S4 or tied to the calibration parameters.

Hydrological simulations of historical and future climate

The calibrated hydrological model was run for the historical simulation period of 1990-2023 using observed climate forcing data (Scharling, 1999a, b; Stisen et al., 2011). Future hydrological projections are derived from simulations using the hydrological model forced by climate model projections, including precipitation, air temperature (T_{air}), and potential evapotranspiration. The resulting impacts on groundwater levels, as simulated by the hydrological model, are evaluated. We used 17 climate models (Table S5) with the Representative Concentration Pathway 8.5 (RCP8.5), which represents the RCP scenario (2.6-8.5) leading to the highest emissions and strongest impact of climate change. The climate model outputs are generated and bias corrected by Pasten-Zapata et al. (2019), and the Global and Regional Circulation (GCM, RCM) models originate from the Euro-CORDEX project (Jacob et al., 2014).

The climate simulations cover three 30-year periods: the reference period (1991-2020), the mid-century (2041-2070) and the end-century (2071-2100). All 51 climate simulations (17 climate models × 3 periods) were first run using the initial potential head from the national model climate simulations (Henriksen et al., 2020). Subsequently, they were rerun using the mean potential head for the respective 30-year period as the initial potential head.

Empirical CO_2 emission models

Implementation of annual CO_2 emission model

Recent studies established a functional relationship between the annual net ecosystem carbon balance (NECB) for CO_2 and the mean annual WTD (Koch et al., 2023; Tiemeyer et al., 2020) by fitting a nonlinear Gompertz function. Like in Koch et al. (2023) and Tiemeyer et al. (2020), this study considers NECB as only CO_2 fluxes, excluding methane (CH_4) and other carbon exports such as dissolved or particulate organic carbon. We apply the WTD functional relationship for CO_2 from Koch et al. (2023), which is fitted to Danish flux data, and refer to it as the *Annual WTD model.* The *Annual WTD model* demonstrates a systematic relationship in which CO_2 flux from NECB increases with annual WTD in the interval between 7 cm and 50 cm, above which an asymptotic level of 10 Mg CO_2-C ha^{-1} yr^{-1} is reached (Koch et al., 2023). The *Annual WTD model* is therefore not sensitive to changes in WTD deeper than approximately 50 cm. At WTD levels less than 7 cm, the *Annual WTD model* suggests CO_2 uptake; however, this element is not included in our analysis which only models CO_2 emission.

Derivation and implementation of daily CO_2 emission model

For our empirical model to predict daily soil CO_2 fluxes (fCO_2) we assume that the WTD dependent NECB (Tiemeyer et al. 2020, Koch et al. 2023) is driven mainly by the response of soil respiration to WTD and T_{air}, as gross primary photosynthesis (GPP) and aboveground autotrophic respiration is mostly dependent on light availability and plant phenology (Rodriguez et al., 2024). This allows scaling to match the NECB magnitude but maintains integrity in the regulation of WTD on soil CO_2 fluxes.

Using a unique and comprehensive coupled dataset (Nielsen et al., 2025a) of daily mean net soil CO_2 fluxes, T_{air} and WTD for six spatial replicate measurement points, we develop a coupled temperature and WTD dependent empirical soil CO_2 flux model, hereafter referred to as the *Daily WTD-T_{air} model*. The model essentially scales the WTD-fCO_2 relation to T_{air}. The dataset Nielsen et al. (2025a) is from a drained fen, called Vejrumbro (Figure 1), with similar characteristics (soil type, climate, land use history) as the peat area in the Tuse Stream catchment (see methodological details in Nielsen et al. (2025a). The soil net CO_2 fluxes, WTD and T_{air} were measured automatically for one year (2022-2023) (Nielsen et al., 2025a) and we used a subset of fluxes measured for six spatial replicates 5-6 times per day, resulting in a dataset of 10950 – 13140 individual fluxes covering 365 days (Nielsen et al., 2025a).

Implementation of CO_2 flux models

Spatially distributed net soil CO_2 fluxes are calculated at a 100-meter scale across the 13 km^2 contiguous peatland area (Figure 1) with the *Annual WTD model* and the *Daily WTD-T_{air} model*, respectively, using WTD at a 100-meter scale (hectare scale) and a uniform T_{air}. Afterwards the spatially distributed soil CO_2 fluxes are aggregated to represent the spatial mean of the 13 km^2 peatland area.

First, we applied the *Annual WTD model* and the *Daily WTD-T_{air} model* for the historical simulation period of 1990-2023, using spatiotemporal distributed WTD from the calibrated hydrological model. Afterwards, the empirical CO_2 models are utilized on each of the 17 climate projections for T_{air} and WTD. Daily T_{air} for the Tuse Stream catchment peatland area is taken directly from the 17 bias corrected climate projections, while daily spatial WTD is a model output from the 17 hydrological simulations, when running the hydrological model with the forcing data (precipitation, temperature and evapotranspiration) from the 17 climate projections. Thereby, we are able to quantify the variability in soil CO_2 flux among the 17 climate projections for each of the simulation periods and among the 30 years within each of the simulation periods.

Design and application of rewetting scenarios

For impact evaluations of peatland management scenarios on the annual CO_2 emissions, we define three rewetting scenarios: A, B and C. These scenarios are implemented through controlled modifications of the simulated WTD in peatland grid cells. This method of representing rewetting scenarios does not involve structural modifications to the hydrological model and assumes changes in WTD without accounting for process-based feedback mechanisms within the coupled surface–subsurface hydrological system. Therefore, the rewetting scenarios cannot be interpreted as real-life management practices. All rewetting scenarios were applied for 1990 to 2023, representing the climatology for this period and generating 34-year time series of rewetted WTD.

The scenarios are meant to illustrate different rewetting impacts on WTD, representing wetter winters (A), uniform shift in WTD (B) and wetter summers (C), but all with the same long-term mean WTD. In Scenario A, the daily groundwater table is elevated when it is above the long-term (34-year) mean water table resulting in unchanged water table levels during summer but an increase in winter. Scenario B uniformly raises the water table by a constant scalar, while Scenario C applies the same scalar increase to water table while simultaneously reducing the annual amplitude by half. The modifications of the simulated WTD are implemented using the following equations:

$$WTD_{i_{rewet\ A}} = \begin{cases} WTD_i, & if\ WTD_i \geq \overline{WTD} \\ WTD_i + 2.5 \cdot (\overline{WTD} - WTD_i), & if\ WTD_i < \overline{WTD} \end{cases} \quad [2]$$

$$WTD_{i_{rewet\ B}} = WTD_i - (\overline{WTD} - \overline{WTD_{rewet\ A}}) \quad [3]$$

$$WTD_{i_{rewet\ C}} = \overline{WTD_{rewet\ B}} + 0.5 \cdot (WTD_{i_{rewet\ B}} - \overline{WTD_{rewet\ B}}) \quad [4]$$

where $WTD_{i_{rewet\ A}}$, $WTD_{i_{rewet\ B}}$ and $WTD_{i_{rewet\ C}}$ is the daily WTD in a grid cell for rewetting scenario A, B and C, respectively. WTD_i is the daily WTD in a grid cell from the calibrated hydrological model. $\overline{WTD}$ is the long-term (34-year) mean WTD in a grid cell from the historical period of the calibrated hydrological model. $\overline{WTD_{rewet\ A}}$ and $\overline{WTD_{rewet\ B}}$ are long-term (34-year) mean WTD in a grid cell from the rewetting scenario A and B, respectively.

Bootstrapping means of future climate CO_2 emissions

We applied a bootstrap resampling approach to estimate the uncertainty in the mean values of soil CO_2 flux. Specifically, we resampled the means over the 17 climate models, each containing 30 annual values, with replacement. This process was repeated 10,000 times to construct bias-corrected and percentile-based 95% confidence intervals around the bootstrapped means.

Results

Hydrological model

Calibration of the hydrological model

The model calibration, running 1000 model evaluations based on three objective function groups, using Ostrich ParaPADDS optimizer with 40 parallel model executions, took ~24 hours on a Xeon Et-4850 @2,20 GHz Server. The calibration resulted in 203 non-dominated solutions forming a three-dimensional pareto front. Figure 2 presents scatterplots of the three objective functions, illustrating the trade-offs between them. Especially, there is a clear trade-off between the two objective functions addressing temporal dynamics (KGE_{WTD}) and spatial dynamics ($r_{spatial}$), as illustrated in Figure 2a.

The number of non-dominated solutions and the trade-offs illustrate that several parameter sets can be considered and that an ensemble of parameter sets could be selected. For the purpose of further analysis and climate change impact assessments, however, we select one balanced solution from the non-dominated solutions, through a stepwise procedure. First, a pre-screening was performed with performance criteria for WTD of KGE_{WTD} larger than 0.6, for discharge of $KGE_{discharge}$ larger than 0.6 and for hydraulic head in deeper wells of ±1 m, for ME_{head} and ME_{amp}, respectively. Afterwards, the balanced parameter set was selected as the solution with the highest spatial correlation ($r_{spatial}$).

The selection procedure was designed to prioritize accurate simulation of the temporal dynamics of peatland WTD, while maintaining strong performance across additional objective functions and maximizing spatial correlation accuracy. Initial calibration efforts indicated that achieving a KGE_{WTD} value greater than 0.6 was necessary to ensure an adequate alignment between the simulated and observed WTD time series.

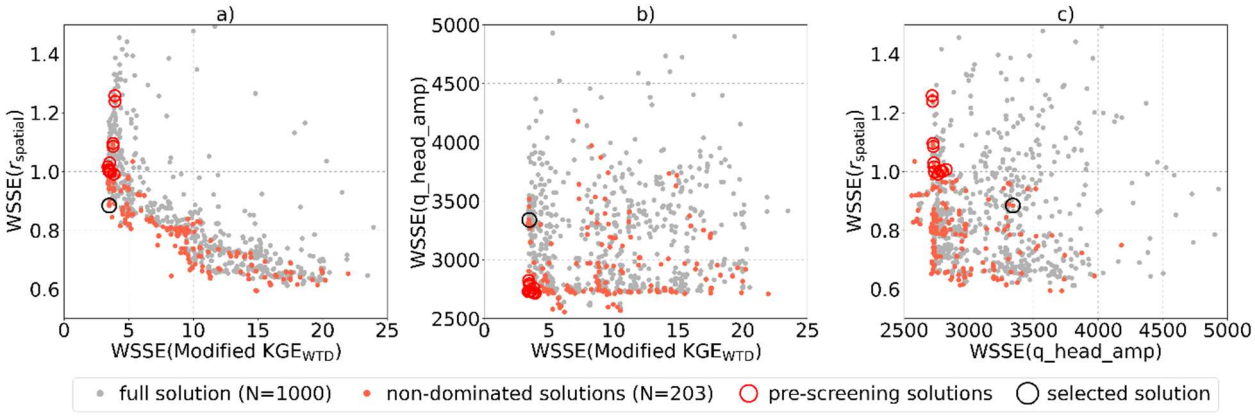

Figure 2: Scatterplots of WSSE (weighted sum of squared errors) for the three objective function groups in the calibration. Pareto front for 1000 model evaluations.

Hydrological model performance

Model performance metrics for the selected solution are summarized in Table 2. The q_head_amp objective function is separated into individual contributions from the metrics KGE_q, ME_{head} and ME_{amp}. Additionally, Table 2 shows the three metrics which make up the modified KGE_{wtd}: r_{wtd}, α_{wtd} and ME_{wtd}. In general, the model performs well with a KGE_{wtd} in peat of 0.64, a KGE_q of 0.63, a ME_{head} for the deep wells of 0.75 m and a ME_{amp} for the deep wells of 0.51 m for the selected solution. However, the correlation coefficient for the spatial variability ($r_{spatial}$) is poor with a value of 0.06. The model optimization achieves solid metrics on all the three components of KGE_{wtd}. The mean bias of WTD across all shallow peatland observation wells (ME_{wtd}) is only 8 cm (Table 2).

Table 2: Hydrological model performance

Name of metric		Abbreviation	Unit	Selected solution
Modified KGE on WTD		$KGE_{WTD_{modified}}$	-	0.64
	Correlation coefficient WTD	r_{WTD}	-	0.83
	Measure of variance	α_{WTD}	-	0.14
	Mean error of WTD	ME_{WTD}	m	0.08
Spatial correlation of the mean WTD		$r_{spatial}$	-	0.06
KGE on discharge		KGE_q	-	0.63
Mean error on the hydraulic heads		ME_{head}	m	0.75
Mean error on amplitude of the hydraulic heads		ME_{amp}	m	0.51

Though the model obtains a relatively small mean error, it largely underestimates the spatial variability in WTD. The observed mean WTD variability across the 22 monitoring wells (SD = 16.5 cm) is considerably higher than that observed in the simulations (SD = 6.8 cm). Even though the model performance on KGE_{WTD} was generally good, it proved difficult to reproduce the spatial variation in mean WTD.

To investigate the underestimation of spatial variability in WTD, we analyzed several spatial variables considered relevant for explaining the observed variability in WTD: peat thickness, topography and proximity to water bodies. However, no clear correlation was found between these spatial variables and the mean observed WTD or model bias, as all had a correlation coefficient smaller than 0.34. See Table S6.

Historical simulations of water table depth

The simulated WTD, generated by the calibrated hydrological model driven by historical climate for the period 1990-2023, adequately represent both the observed seasonal patterns of WTD and their short-term responses to precipitation events. Figure 3 shows the time series of WTD from two individual monitoring wells as a typical example of the temporal match between observed and simulated WTD.

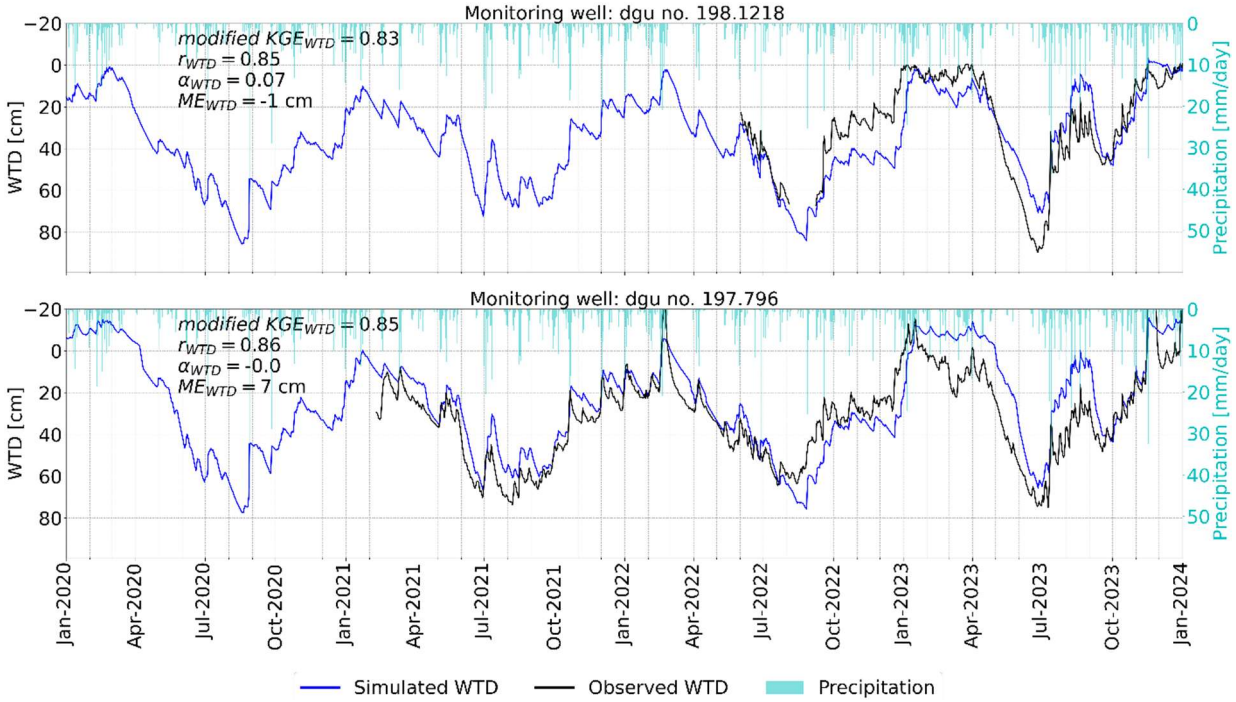

Figure 3: Example of observed and simulated timeseries for water table depth (WTD) for monitoring wells dgu no. 198.1218 and dgu no. 197.796. Including metrics for these wells.

Meteorological climate predictions

Changes in precipitation, temperature and evapotranspiration patterns in future climate projections for Denmark generally indicate an increase in both temperature and annual precipitation. Table 3 presents the mean air temperature, mean annual precipitation and mean potential evapotranspiration derived from the 17 climate projections across the three simulation periods.

Table 3: Mean ± SD (n=17) of annual air temperature, precipitation and potential evapotranspiration from the 17 climate models during the three simulation periods.

	Unit	Reference period (1991-2020)	Mid-century period (2041-2070)	End-of-century period (2071-2100)
Mean annual air temperature	◦C	8.9 ± 0.7	10.6 ± 0.8	12.1 ± 0.8
Mean annual precipitation	mm yr^{-1}	780 ± 121	837 ± 130	906 ± 152
Mean annual potential evapotranspiration	mm yr^{-1}	621 ± 25	678 ± 27	727 ± 27

Hydrological climate predictions

Climate simulations using the hydrological model indicate a decreasing trend in mean annual WTDs (Table 4), resulting in a shallower annual mean groundwater table in future climate conditions. Both summer and winter mean WTDs are projected to be closer to the surface, suggesting generally wetter conditions. The mean annual amplitude of WTD remains unchanged under future climate scenarios (Table 4), indicating that there is no greater seasonal drawdown of the water table during summer, although the duration of the drawdown period may be extended.

Table 4: Statistics of WTD when using the hydrological model for climate simulations. Mean ± SD (n=17) over the 17 climate models during the three simulation periods. Summer is June, July and August, Winter is December, January and February. The amplitude is based on the monthly means of WTD to avoid outliers.

	Unit	Reference period (1991-2020)	Mid-century period (2041-2070)	End -of-century period (2071-2100)
Mean annual WTD	cm	31 ± 1	27 ± 2	24 ± 3
Mean summer WTD	cm	47 ± 1	40 ± 3	34 ± 3
Mean winter WTD	cm	18 ± 2	14 ± 4	10 ± 3
Mean annual WTD amplitude	cm	51 ± 2	50 ± 4	52 ± 4

Derivation of empirical daily soil CO_2 flux model

An analysis of the Vejrumbro dataset indicated a clear temperature dependency on the relation between soil CO_2 flux (fCO_2) and WTD. The Vejrumbro dataset was resampled to daily means of WTD, T_{air} and soil CO_2 flux across the six spatial replicate measurement points omitting data from days with less than 24 flux measurements. This resulted in a dataset with 231 daily observations for each of fCO_2, WTD and T_{air} distributed evenly over a year. Traditionally, empirical emission models for ecosystem respiration (R_{eco}) are fitted to soil temperature. However, due to the strong linear relationship between daily soil temperature and daily air temperature at the Vejrumbro site ($r = 0.96$, p-value < 0.001) (Figure S4), T_{air} was used as a proxy for soil temperature when fitting the *Daily WTD-T_{air} model.* This use of air temperature also facilitates upscaling and omits the need for projecting soil temperatures under climate change scenarios.

To investigate how the WTD-fCO_2 relation scales with temperature, we binned daily soil CO_2 flux into five temperature intervals: <4°C (n=39), 4-8°C (n=32), 8-12°C (n=52), 12-16°C (n=70) and >16°C (n=38) and applied a linear regression model ($y=ax$) with the intercept constrained at zero within each temperature bin. The regressions were constrained to pass through the origin, reflecting the

assumption that soil CO_2 flux is zero when the WTD is zero. Thereby, the relationship between fCO_2 and WTD within each temperature bin was modeled using a linear regression of the form:

$$fCO_2 = a \cdot WTD \quad [5]$$

where fCO_2 represents soil CO_2 flux [Mg CO_2-C ha^{-1} day^{-1}], a denotes the fitted slope and WTD is water table depth [cm], with positive values indicating depths below the surface.

This analysis revealed an increasing slope, i.e. sensitivity of soil CO_2 flux to changes in WTD, with rising temperature (Figure S5 and Figure 4a), indicating that the WTD- fCO_2 slope (a) can be modelled as a linear function of temperature (T_{air}) (Figure 4b):

$$a = b \cdot T_{air} + c \quad [6]$$

Combining these relationships yields a simple model of the soil CO_2 flux:

$$fCO_2 = b \cdot T_{air} \cdot WTD + c \cdot WTD \quad [7]$$

where T_{air} [◦C] is the temperature, b [Mg CO_2-C ha^{-1} day^{-1} cm^{-1} ◦C^{-1}] and c [Mg CO_2-C ha^{-1} day^{-1} cm^{-1}] are empirical constants.

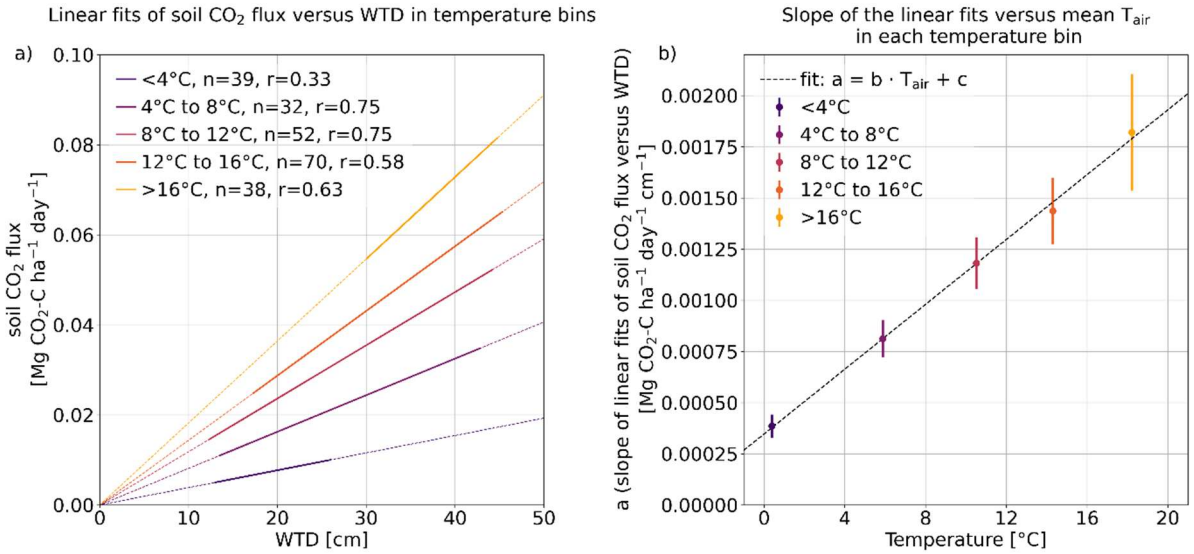

Figure 4: Left: linear models of soil CO_2 flux vs. water table depth (WTD) in air temperature bins. The thicker segment of the line represents the range of data used to derive the fitted model. n is the number of daily observations of soil CO_2 flux in each temperature bin. r is Person correlation coefficient. Raw data behind the linear regressions can be seen at Figure S5. Right: Slope (incl. uncertainty) (of the linear fit of soil CO_2 flux versus WTD) versus observed mean temperature in each temperature bin.

Having established a suitable form of the empirical soil CO_2 flux equation, we used nonlinear least squares fit to estimate the b and c parameters based on the daily soil CO_2 flux, T_{air} and WTD (without temperature bins). This method minimizes the residual sum of squares between the observed soil CO_2 flux and the *Daily WTD-T_{air} model*. The resulting fitted model demonstrated a significant correlation to the observed data ($r = 0.78$, p-value < 0.001, RMSE = 0.021 Mg CO_2-C ha^{-1} day^{-1}) (Figure S6) with daily soil CO_2 flux increasing in response to rising WTD and T_{air} (Figure S7). The fitted empirical constants are as follows: $b = 8.32 \cdot 10^{-5}$ Mg CO_2-C ha^{-1} day^{-1} cm^{-1} ◦C^{-1}, $c = 3.33 \cdot 10^{-4}$ Mg CO_2-C ha^{-1} day^{-1} cm^{-1}.

The *Daily WTD-T_{air} model* predicts the highest soil CO_2 flux under conditions of simultaneously high T_{air} and WTD, where a high WTD refers to a water table located furthest below the surface (dry conditions). The multiplicative *Daily WTD-T_{air} model* demonstrated a moderate fit to the soil CO_2 flux data, with a R^2 of 0.61. To assess the individual contributions of the predictor variables, we also

computed the R^2 between CO2 flux and T_{air} and WTD separately. This was done using a constructed dataset that included all combinations of WTD and T_{air} within the model range. This resulted in R^2 values of 0.34 for T_{air} and 0.54 for WTD (Table S7). These values reflect the explanatory power of each variable in isolation.

Despite the significant variability in the observed net ecosystem carbon balance (NECB) used for the *Annual WTD model* (Figure 5) it is considered to represent a robust mean as it is based on multiple sites and years for Danish and German conditions. Compared to the *Annual WTD model* both the measured soil CO_2 flux (12.9 Mg CO_2-C ha^{-1} yr^{-1} (green circle)) and the *Daily WTD-T_{air}* simulated soil CO_2 flux (13.6 Mg CO_2-C ha^{-1} yr^{-1} (not shown)) at Vejrumbro are above the corresponding fitted value of NECB (8.7 Mg CO_2-C ha^{-1} yr^{-1} (orange circle)) based on an annual WTD of 29 cm, but still within the range of observed NEBCs used for fitting the *Annual WTD model* (Figure 5). This may be explained by the methodology of flux measurements at Vejrumbro that did not consider GPP (CO_2 uptake) and therefore are expected to result in higher net CO_2 fluxes. In order to align the *Daily WTD-T_{air} model* to the level of the *Annual WTD model* where GPP is included, a scaling factor based on the above differences ($f_{scaling}$ = 0.64) was applied to equation 7 to account for lack of GPP in the soil CO_2 fluxes used for empirical model development. Applying this scaling factor, we seek to avoid the risk of overestimating emissions when applying the *Daily WTD-T_{air} model* at other locations.

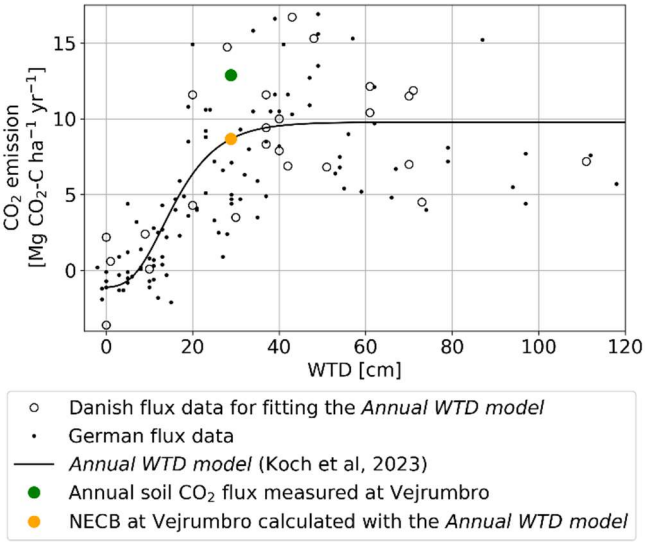

Figure 5: The Annual WTD model together with the Danish flux data of annual NECB and WTD data underlaying the model (Koch et al., 2023). *German flux data are included for comparison (Tiemeyer et al., 2020). Colored circles are measured and calculated soil CO_2 flux and NECB for the Vejrumbro dataset, so the colored circles represent the year 2022-2023.*

The Vejrumbro dataset used for fitting the *Daily WTD-T_{air} model* was limited to a maximum WTD of 47 cm and maximum T_{air} of 21°C (Figure S7). Outside this range, the predictions of the *Daily WTD-T_{air} model* exhibits increased uncertainty. At the same time, it is generally understood that the upper portion of the peat layer drives the net CO_2 emissions observed at the surface. Therefore, the extrapolation of WTD in the *Daily WTD-T_{air} model* must be constrained. The *Daily WTD-T_{air} model* should be sensitive within a WTD range comparable to the expected daily variation in the *Annual WTD model*, which also reaches an fCO_2 asymptotic at deeper water tables. In the *Annual WTD model*, the Annual NECB reaches 90% of its maximum asymptotic level at a mean annual WTD of 30 cm (Figure 5). The mean annual WTD results from intra-annual (within year) WTD variation described by the annual amplitude. The mean annual amplitude (based on monthly means) is 65 cm, across the 22 observed WTD time series in the Tuse Stream catchment used for calibrating the hydrological model. We assume that a mean annual WTD of 30 cm originates from an annual WTD variation with a similar

amplitude. Therefore, we assume that the WTD range of the *Daily WTD-T_{air} model* is 30 + 65/2 cm = 62.5 cm. For the T_{air} range, it is assumed that the sensitivity continues until 25°C, which is a daily average value very rarely occurring, even in future climate projections. Thus, when applying the *Daily WTD-T_{air} model,* daily WTD values and T_{air} values were truncated, setting WTD and T_{air} to 62.5 cm and 25°C, respectively, when exceeding those thresholds.

In both the *Daily WTD-T_{air} model* and *the Annual WTD model,* CO_2 fluxes are constrained so that the model does not simulate negative fluxes or carbon uptake(Gyldenkærne et al., 2025).

CO_2 emissions from peatlands

CO_2 emissions throughout the historical simulation period

The long-term mean of the emission factor for the Tuse Stream catchment peat area is 8.0 ± 0.8 Mg CO_2-C ha^{-1} yr^{-1} (mean ± SD, n=34) when using the *Annual WTD model* and 8.8 ± 1.6 Mg CO_2-C ha^{-1} yr^{-1} (mean ± SD, n=34) when using the *Daily WTD-T_{air} model* (Table 5).

Table 5: Long-term mean water table depth (WTD), long-term mean annual WTD amplitude (based on monthly means of WTD to avoid outliers) and long-term soil CO_2 flux, throughout the historical period and the three modified 34-year WTD time series of rewetting scenarios. Mean ± SD is based on the 34 years of the historical period (1990-2023).

	Unit	Historical period (1990-2023)	Rewetting scenario A	Rewetting scenario B	Rewetting scenario C
Mean WTD	cm	34 ± 8	14 ± 18	14 ± 8	14 ± 4
Mean annual WTD amplitude	cm	51 ± 11	110 ± 28	51 ± 11	26 ± 5
CO_2 emission from *Daily WTD-T_{air} model* aggregated to annual	Mg CO_2-C ha^{-1} yr^{-1}	8.8 ± 1.6	7.7 ± 2.0	5.2 ± 1.5	4.4 ± 0.8
CO_2 emission from *Annual WTD model* aggregated to annual	Mg CO_2-C ha^{-1} yr^{-1}	8.0 ± 0.8	4.6 ± 3.0	4.3 ± 2.0	4.4 ± 1.2

Figure 6 shows T_{air}, as wells as the spatial mean of WTD and CO_2 emissions across the peatland, as simulated by the *Daily WTD-T_{air} model* and the *Annual WTD model* during the historical period. The CO_2 emissions calculated with the *Daily WTD-T_{air} model* (red line in Figure 6c, 6d) depend on both the observed daily temperature variability (orange line in Figure 6a) and simulated intra-annual (seasonal) WTD variability (blue line in Figure 6b), while the CO_2 emission calculated with the *Annual WTD model* (black points in Figure 6d) only depends on the inter-annual (annual means) WTD (blue points in Figure 6b) and not the temperature.

Inter-annual (between years) variation in CO_2 emission is substantially larger when using the *Daily WTD-T_{air} model* (SD = 1.6 Mg C-CO_2 ha^{-1} yr^{-1}) compared to the *Annual WTD model* (SD = 0.8 Mg C-CO_2 ha^{-1} yr^{-1}) (Figure 6d), as the former captures extreme events, such as periods of high temperature or deep groundwater tables, as well as compound events involving the simultaneous occurrence of both. In contrast, the *Annual WTD model* is insensitive to temperature and the intra-annual (within year) timing of deep WTD. Moreover, the *Annual WTD model* imposes an upper limit of 10 Mg CO_2-C ha^{-1} yr^{-1} for annual emissions (Koch et al., 2023) (Figure 5). During the summer of 2018, a compound extreme event occurred, characterized by both high temperatures and deep groundwater table. The annual CO_2 flux for this year shows a 34% increase when estimated using the *Daily WTD-T_{air} model* compared to the *Annual WTD model*. This discrepancy arises from the *Daily WTD-T_{air} model's* ability to account for the prolonged duration of concurrent high temperatures and deep groundwater table conditions throughout the summer (Figure 6d). Conversely, in 2010, the *Daily WTD-T_{air} model* estimates significantly lower annual CO_2 emissions compared to the *Annual WTD model* (Figure 6d). This difference is due to the emission model's ability to account for the effects of prolonged periods of low temperatures during the autumn and spring of 2010, leading to a mean annual temperature below

the long-term mean, despite summer temperatures being consistent with other years (Figure 6a). Examples of years with extreme events primarily driven by either WTD or T_{air} include 1996, which experienced a significant summer decline in groundwater table (Figure 6b), and 1997, which was characterized by elevated summer temperatures (Figure 6a). However, neither of these events led to CO_2 emissions as high as those simulated during the compound event of both high temperatures and deep water table in 2018 (Figure 6).

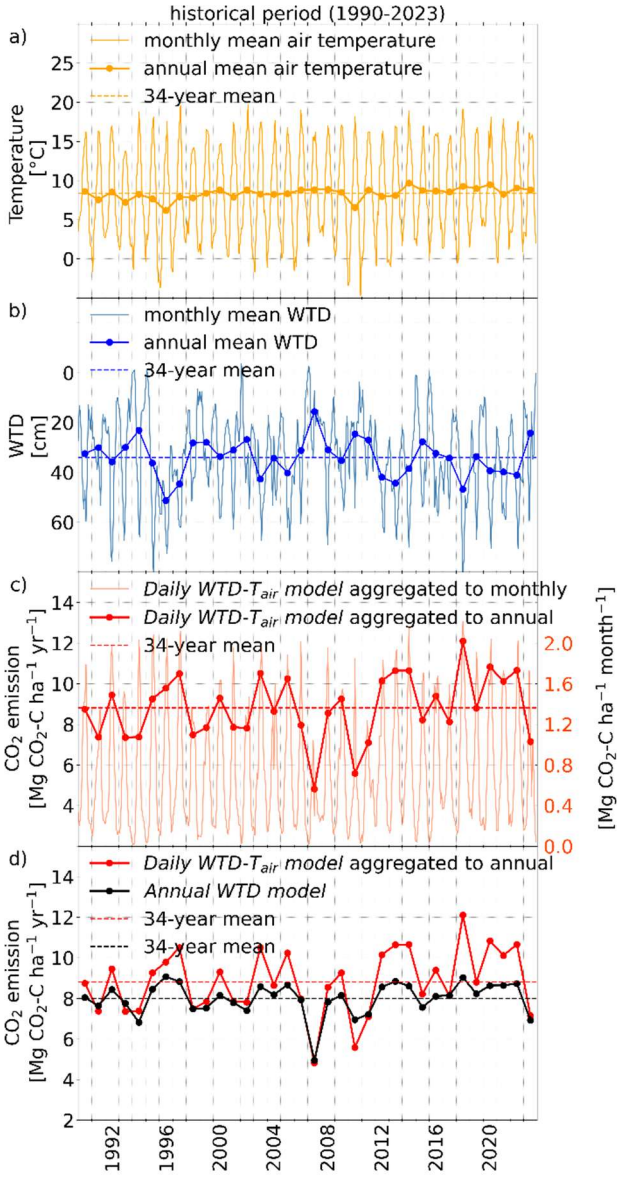

Figure 6: Air temperature (T_{air}), water table depth (WTD) and soil CO_2 emission for the historical simulation period 1990-2023.

CO_2 emissions under different rewetting scenarios

The rewetting scenarios represent an adjustment to the WTD simulated by the hydrological model over the 34-year historical period, thereby reflecting the climatological conditions prevailing during that time. Across all three rewetting scenarios, the long-term (34-year) mean WTD was raised by 20 cm, from 34 cm to 14 cm below the surface, ensuring a consistent long-term annual mean WTD among the rewetting scenarios (Table 5). Accordingly, the application of the *Annual WTD model* for estimating CO_2 fluxes result in CO_2 emissions between 4.3 ± 1.2 Mg C-CO_2 ha^{-1} yr^{-1} (mean ± SD, n=34) and 4.6 ± 3.0 Mg C-CO_2 ha^{-1} yr^{-1} (mean ± SD, n=34) across all rewetting scenarios (Table 5). The mean annual soil CO_2 flux from the three rewetting scenarios, as calculated using the *Annual WTD model,* are similar but not

identical. This is because the *Annual WTD model* is applied to each of the 34 individual annual mean WTD values rather than to a single long-term mean WTD. The SD of CO_2 emissions calculated using the *Annual WTD model* in scenario C is markedly lower than in rewetting scenario A and B, reflecting the lower inter-annual (between years) variability in mean annual WTD observed for this scenario (Table 5).

In contrast to the *Annual WTD model*, the *Daily WTD-T_{air} model* captures the simultaneous occurrence of low groundwater table and high T_{air} during the summer months. Application of this emission model indicates that raising the groundwater table during summer months (rewetting scenario C) yields the greatest reduction potential in soil CO_2 emissions (Table 5), leading to a 50% decrease in the mean value, from 8.8 ± 1.6 to 4.4 ± 0.8 Mg C-CO_2 ha^{-1} yr^{-1} (mean ± SD, n=34) (Table 5). In contrast, management scenarios that primarily target increase in winter water table (rewetting scenario A) exhibit only marginal emission reduction potential (Table 5).

A visual representation of daily soil CO_2 emissions in relation to mean daily temperature during the 34-year historical period under different WTD conditions (Figure 7) reveals that high summer temperatures are a key driver of CO_2 emissions. WTD observations from the Tuse catchment peatland indicate that, during shorter periods in the warm summer months, the WTD can exceed 80 cm (Figure 3). These periods with very low summer water table contribute substantially to total CO_2 emissions (Figure 7).

A rewetting scenario that mainly generates wetter winter conditions (rewetting scenario A) has very limited CO_2 emission reduction. All three scenarios assume that even under rewetting, the peatland WTD will follow a climate driven seasonality and that obtaining zero WTD in summer periods will be difficult by classical nature-based solutions. Rewetting scenario C, which features the greatest increase in summer WTD, achieves the largest reduction in CO_2 emissions (Figure 7). Permanent wet conditions with WTD at zero would be required to obtain zero CO_2 emission with the developed *Daily WTD-T_{air} model,* but under such conditions, methane emissions would also come into play and plant growth would be severely limited.

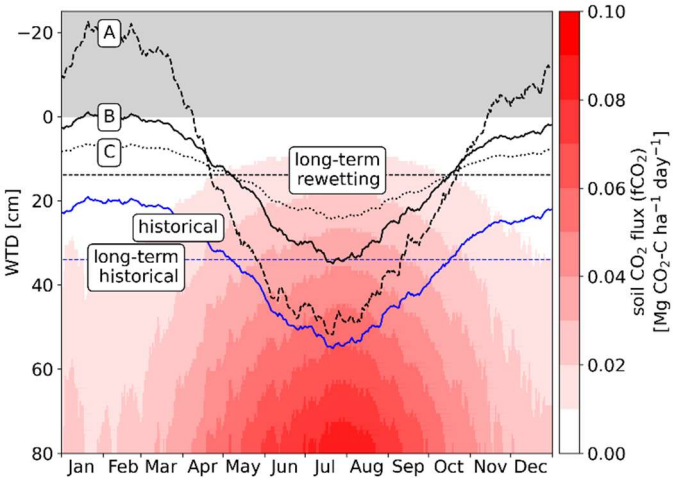

Figure 7: Colormap: Visual representation of the annual distribution of daily surface soil CO_2 flux (fCO_2, CO_2 exchange with atmosphere) under mean daily temperature during the historical period (1990-2023) and for different water table depths (WTD). Curves: solid blue line: simulated daily mean WTD during the historical period and corresponding long-term (34-year) mean WTD, black lines: daily mean WTD for each of the modified 34-year WTD time series of rewetting scenarios (A, B and C) and the corresponding long-term (34-year) mean WTD.

CO_2 emissions across future climate simulation periods

Figure 8 shows the same variables as Figure 6 but based on a representative climate model simulation instead of the observed climate record, offering a typical example of the development of temperature,

WTD and soil CO_2 flux through the reference, mid-century and end-of-century periods based on the RCP 8.5 pathway.

The future climate simulations show an increase in both the annual mean temperature and groundwater levels combined with higher maximum summer temperature (Figure 8a, 8b, Table 3, Table 4). The bootstrap mean of soil CO_2 flux calculated with the *Annual WTD model* over all climate models predicts a decreasing trend in soil CO_2 flux under future climate conditions (Figure 9a, horizontal dotted black line in Figure 8d), driven by an inter-annual (between years) mean WTD closer to surface (Table 4, Figure 8b). However, this decreasing trend is countered by the inclusion of T_{air} effects when applying the *Daily WTD-T_{air} model* (Figure 9b, horizontal dotted red line in Figure 8c and 8d*)*.

The wider confidence intervals in the mean annual CO_2 emissions for the future periods with both CO_2 emission model (Figure 9) indicate that the inter-annual (between years) soil CO_2 fluxes become more variable in future climate. Furthermore, the confidence intervals for the individual periods are wider for the *Daily WTD-T_{air}* (Figure 9b) compared to the *Annual WTD model* (Figure 9a), which is expected as variations in T_{air} and not only WTD is included as with the *Daily WTD-T_{air} model*. This demonstrates that the *Daily WTD-T_{air} model* captures extreme events, including periods of high temperature or deep groundwater table, whether these events occur simultaneously (compound event) or independently.

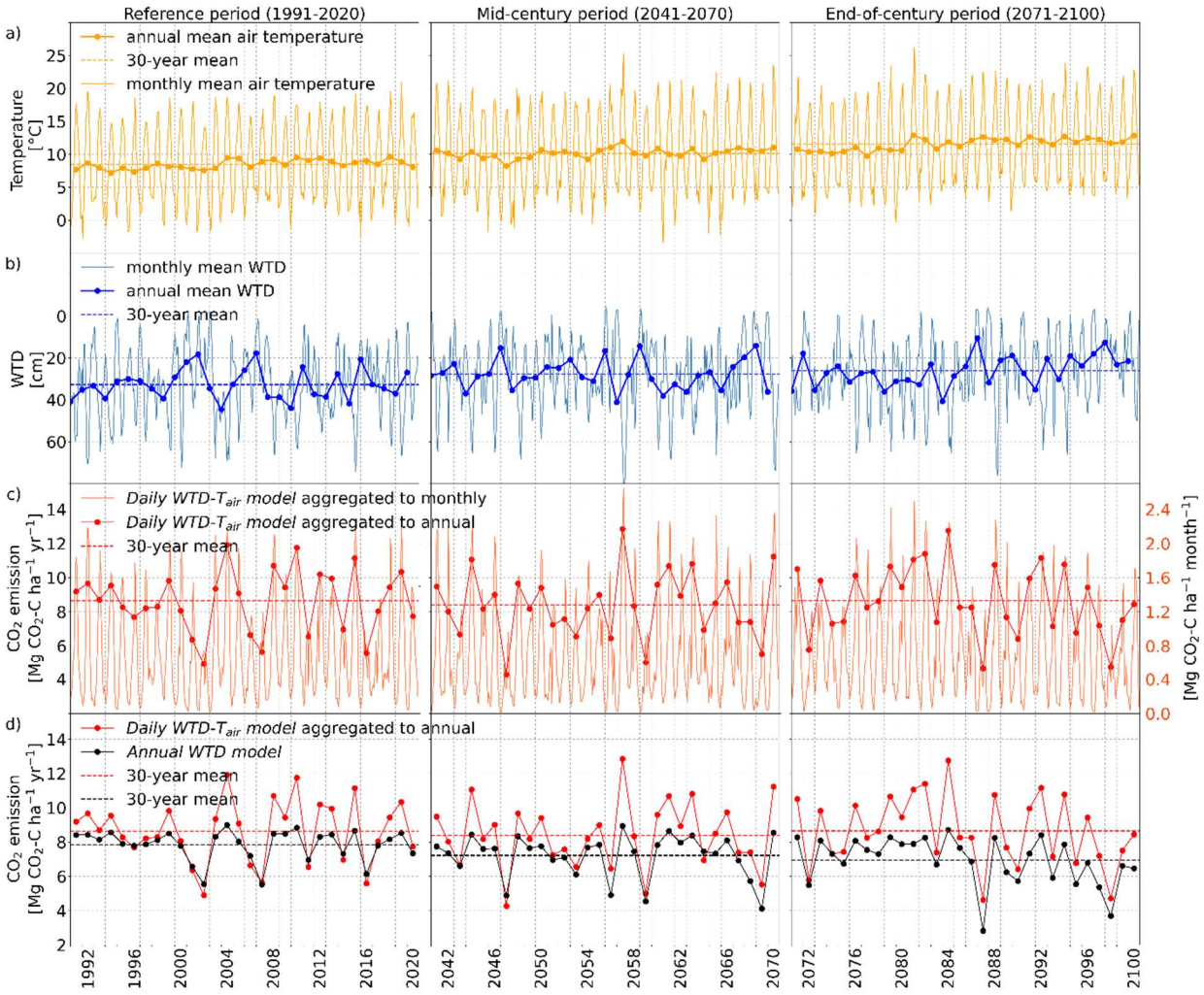

Figure 8: Example of air temperature (T_{air}), water table depth (WTD) and soil CO_2 flux for future climate simulation with climate model projection no. 5 (Table S6).

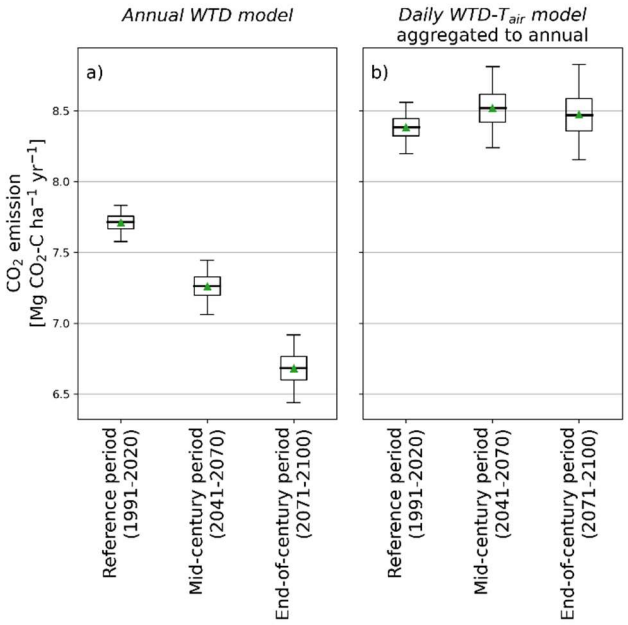

Figure 9: Boxplot showing the distribution of bootstrap means of soil CO_2 emissions according to the Daily WTD-T_{air} model and Annual WTD model during future climate. Green triangles and horizontal lines indicate the mean and the median of the bootstrap mean, respectively. Boxes show the 25th and 75th percentiles. Whiskers indicate the 95% confidence intervals. Outliers are not shown.

The results presented in Figure 9 suggest that the impact on CO_2 emissions caused by future increases in T_{air} and increases in water tables cancel each other out when using the *Daily WTD-T_{air} model*. To investigate this further, we analyze how the combination of T_{air} and WTD shift between the reference and the end-of-century periods, despite relatively stable total CO_2 emission.

We wish to identify the specific combination of T_{air} and WTD that are associated with the majority of the CO_2 emission. Due to the non-linear response of soil CO_2 flux to environmental drivers in the *Daily WTD-T_{air} model*, a large fraction of total emissions is generated on relatively few days. To quantify this, we calculated p50, defined as the proportion of days required to account for 50% of the total annual soil CO_2 flux (fCO_2). This was achieved by ranking the daily values of fCO_2, WTD, and T_{air} in ascending order according to fCO_2. Subsequently, the ranked fCO_2 values were cumulatively summed to obtain their percentile distribution (Figure S8). The procedure was first applied to fCO_2, WTD, and Tair data from the historical simulation period, with the resulting percentile curves shown in Figure S8. Over the historical simulation period, 50% of the total fCO_2 ($fCO_{2,\,p50}$) was generated within 22% of the days (p50 = 22%), while the value of $fCO_{2,\,p50}$ and corresponding WTD_{p50} and $T_{air,\,p50}$ are estimated to be $4.15 \cdot 10^{-2}$ g CO_2-C ha^{-1} day^{-1}, 47 cm and 13.8 °C (Table 6 and Figure S8).

Similar estimates are derived from the three timeslots from the climate models (reference, mid-century and end-of-century climate simulation periods) using the 17 different climate models. For the future, 50% of the total fCO_2 is expected to occur within approximately 21 ± 1 % (mean ± SD, n=17) of the days (Table 6). The daily soil CO_2 flux associated to p50 ($fCO_{2,\,p50}$) and p50 are nearly identical across both the historical and future climate simulations periods (Table 6). As also shown in Figure 9b, the magnitude and temporal distribution of fCO_2 are predicted to remain unchanged in the future. While the value of $fCO_{2,\,p50}$ remains relatively constant around $4 \cdot 10^{-2}$ Mg CO_2-C ha^{-1} day^{-1} for future climate periods, the corresponding WTD_{p50} and $T_{air,\,p50}$ values change as a result of changing climate moving towards higher temperatures (17 °C) and shallower groundwater table (40 cm).

Figure 10 provides a graphical representation of fCO_2 obtained from the *Daily WTD-T_{air} model*, with the colormap illustrating the daily fCO_2 corresponding to different combinations of T_{air} and WTD. The daily

$fCO_{2,\,p50}$ ($4.15 \cdot 10^{-2}$ g CO_2-C ha^{-1} day^{-1} for the historical period (Table 6)) can be achieved through various combinations of T_{air} and WTD (dark red dotted line in Figure 10). The values of $T_{air,\,p50}$ and WTD_{p50} corresponding to $fCO_{2,\,p50}$ for the Tuse Stream catchment peatland are plotted as a dark red point. As expected, the $fCO_{2,\,p50}$ values for the reference periods of the 17 climate models (green crosses at Figure 10) are closely aligned with that of the historical period. It is evident that the $fCO_{2,\,p50}$ values for the end-of-century climate conditions (blue crosses at Figure 10) shift along the direction indicated by the pink arrow (along the red dotted line), reflecting a trend toward higher temperatures and lower WTD (i.e. water levels closer to the surface surface). This indicates that the mean daily fCO_2 (Table 6) and the long-term fCO_2 remains constant in the future (Figure 9b), as a result of a counterbalance between impacts of rising temperatures and rising groundwater levels.

The pink arrow at Figure 10 illustrates the characteristic impact of climate change in Denmark, reflecting the concurrent increase in air temperature and shallow groundwater levels (Schneider et al., 2022). In contrast, other regions in Europe are experiencing declining groundwater level trends to climate change (Wunsch et al., 2022). Consequently, CO_2 emissions from peatlands in these regions are expected to shift in the direction indicated by the yellow arrow in Figure 10, towards considerably larger emission rates.

Table 6: p50 is the fraction of days required to reach 50% of the total soil CO_2 flux (fCO_2). $fCO_{2,\,p50}$ is the daily soil CO_2 flux associated with p50. WTD_{p50} and $T_{air,\,p50}$ are the water table depth (WTD) and air temperature (T_{air}) corresponding to $fCO_{2,\,p50}$, respectively. Mean ± SD is based on 17 climate model simulations.

		Historical simulation period	Climate simulation periods		
	Unit	(1990-2023)	Reference period (1991-2020)	Mid-century period(2041-2070)	End-of-century period (2071-2100)
p50	% days	22	21 ± 1	21 ± 1	21 ± 1
$fCO_{2,\,p50}$	Mg CO_2-C ha^{-1} day^{-1}	$4.15 \cdot 10^{-2}$	$4.03 \cdot 10^{-2} \pm 9.89 \cdot 10^{-4}$	$4.00 \cdot 10^{-2} \pm 3.24 \cdot 10^{-3}$	$4.03 \cdot 10^{-2} \pm 3.65 \cdot 10^{-3}$
$T_{air,\,p50}$	°C	13.8	14 ± 0.3	15 ± 0.6	17 ± 1.0
WTD_{p50}	cm	47	46 ± 1	42 ± 3	40 ± 3

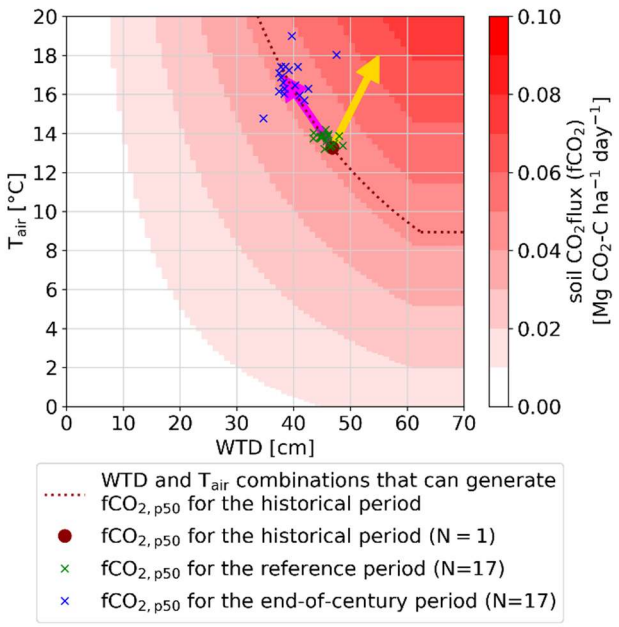

Figure 10: Colormap: Visual representation of the Daily WTD-T_{air} model output, illustrating soil CO_2 flux (fCO2) as function of daily water table depth (WTD) and air temperature (T_{air}). The dark red dotted line represents combinations of T_{air} and WTD that corresponds fCO_2 at p50 ($fCO_{2,\,p50}$), where p50 is the fraction of days required to reach 50% of the total accumulated fCO_2 during the historical period. Green crosses are $fCO_{2,\,p50}$ for the reference period of the 17 climate simulations. Purple crosses

are $fCO_{2,\ p50}$ for the end-of-century climate simulation period of the 17 climate simulations. The pink and yellow arrows indicate different future trends in T_{air} and WTD and the associated trend in CO_2 emissions under climate change. Specific to Denmark, the pink arrow indicates increases in T_{air} and decrease in WTD, other regions might experience increase in both T_{air} and WTD and an associated large increase in CO_2 emissions (yellow arrow).

Discussion

Peatland management under changing climate

In 2023, CO_2 emissions from drained organic soils in croplands and grasslands was estimated to have accounted for 6.7% of Denmark's total emissions, including those from the Land Use, Land-Use Change and Forestry (LULUCF) sector (Nielsen et al., 2025b). Returning peatland organic soils to their natural hydrological state is a cost-effective GHG reduction strategy (IPCC, 2014; Kirpotin et al., 2021; Tanneberger et al., 2021; Wilson et al., 2016). Therefore, national policies (Regeringen, 2024) and the European Union's Nature Restoration Law (Regulation (EU) 2024/1991, 2024) seek to improve the management of peatlands and achieve climate neutrality targets under the urgent Green Transition agenda. To mitigate agricultural GHG emissions Danish ministerial agreements were initiated in 2024, targeting the restoration of 140,000 hectares of peatland (Regeringen, 2024). However, there is a need to strengthen the scientific evidence for mitigation measures to facilitate cost-effective policies. Quantitative predictions of fluxes such as the numbers presented in this study, supports prioritization and design of peatland rewetting strategies by estimating their CO_2 emission reduction potentials accounting for future climate variability impact on CO_2 emissions.

Integration of the process-based hydrological model of the Tuse Stream catchment with the empirically derived *Daily WTD-T_{air} model* of soil CO_2 flux developed in this study revealed that emission simulations at daily timesteps produce greater variability in soil CO_2 fluxes compared to emission estimates derived from annual WTD means. This increased variability is attributed to the daily model's ability to account for short-term compound events, especially the simultaneous occurrence of elevated air temperatures and low groundwater levels.

More importantly, incorporating temperature dependence and higher temporal resolution into the CO_2 emissions model significantly alters the projected trends of CO_2 emission under both rewetting and changing climate conditions.

Nature-based approaches represent the most common real-world rewetting strategies, aiming to restore peatlands towards their natural hydrological regime. At a minimum, such rewetting requires terminating tillage activities and eliminating artificial drainage for instance by blocking of drainpipes and ditches. The rewetting scenarios implemented in this study, represented as simple modifications to WTD, are not reflective of practical management interventions - except perhaps in a few rare and costly restoration projects that involve installing artificial impermeable membranes along peatlands edges (Naturstyrelsen, 2022). However, the outcome of this study can serve as a reference for discussions on realistic expectations on CO_2 emission reductions from rewetted peatlands.

The rewetting analyzed in this study showed how different rewetting scenarios with varying seasonal amplitudes in WTD suggest significantly different emission reduction potential even with identical annual mean WTD. The results illustrate that increasing the groundwater table during warm periods is key to obtaining CO_2 emission reductions, whereas rewetting strategies that mainly raise winter water table without significantly affecting the summer levels offer limited mitigation benefits. This highlights the importance of not only targeting annual reductions in WTD but particularly designing rewetting strategies to increase the summer water table and avoid critically low water levels during droughts and warm periods. Achieving such rewetted conditions may include larger forced control of WTD than what is currently being practiced for most existing rewetting schemes, where the WTD remain subject to climate seasonality impact. Such nature-based solutions are not likely to reduce CO_2 emissions to the degree that current emission reduction policies target.

Also, projections of CO_2 emissions under different climate change scenarios were altered greatly by introducing temperature sensitivity and enhanced temporal resolution into the CO_2 emissions modeling framework. Here our results show that, while the projected rise in groundwater tables in isolation would lead to lower CO_2 emissions in future (when using the *Annual WTD model*), the *Daily WTD-T_{air} model* revealed that anticipated increases in T_{air} are likely to cancel out these reductions, resulting in CO_2 emissions on a level comparable to current levels. This is an important finding, since it suggests that increasing temperatures alone will likely increase CO_2 emissions, and that water level rise driven by climate change or rewetting initiatives might just counteract this trend. Rewetting measures would need to be substantially intensified to ensure climate resilience and achieve meaningful reductions in CO_2 emissions. Additionally, outside the specific case of Danish peatlands located in a region that is susceptible to a future wetter climate, other regions might project both increasing temperatures and lower groundwater tables, and in such cases climate change will significantly increase emissions without any rewetting. We acknowledge that the chosen Representative Concentration Pathway (RCP8.5) represents the scenario leading to the strongest impact of climate change and that additional, milder climate scenarios could have been included.

Hydrological simulation of groundwater levels in peat soil with process-based models

Existing large scale CO_2 emission estimates, such as national inventories from organic soils (Gyldenkærne et al., 2025; Nielsen et al., 2025b), typically combine empirical emission models and data-driven ML approaches for estimating annual WTD (Bechtold et al., 2014; Koch et al., 2023; Tiemeyer et al., 2020). These approaches appear robust and suited for upscaling but are limited in their ability to represent the impact of sub-annual variability in temperature and WTD, which are issues that become increasingly important when analyzing effects of rewetting and climate change. In contrast to most data-driven approaches, hydrological models enable a climate-driven representation of WTD temporal dynamics and the underlying hydrological processes. Moreover, the use of physically based hydrological models has the distinct advantage of enabling scenario-based analyses, such as the evaluation of alternative land use strategies and the projection of future hydrological conditions under climate change scenarios. Utilizing hydrological models that generate high-resolution time series of WTD, it is possible to quantify impacts of WTD dynamics, including water levels, temporal variability and seasonal amplitudes, on changes in CO_2 emissions.

That said we acknowledge that the rewetting scenarios in the present study are applied using simplified adjustments to the simulated WTD, rather than being modeled through a detailed, process-based hydrological framework. Ideally, future assessments should apply catchment-scale models to evaluate peatland management interventions, such as rewetting, thereby enabling analysis of their broader hydrological impacts, including effects on streamflow and groundwater levels in neighboring areas.A unique feature of the present study is that the hydrological model of Tuse Stream catchment is developed in the same modelling framework as the National Hydrological Model of Denmark (Henriksen et al., 2020; Stisen et al., 2019). The National Hydrological Model is continuously updated with new data and operates in near real-time. This integration enables a link between the lessons learned from the Tuse Stream catchment-scale model and the National Hydrological Model of Denmark, thereby improving the representation of peatland hydrology and contributing to the refinement of future national GHG inventories.

As a continuation of this study, we will further investigate the spatial variability of WTD and extent hydrological model to include additional peatland-dominated catchments. Additionally, we will utilize the National Hydrological model to simulate WTD across all Danish peatlands.

Selection, fit and transferability of daily CO_2 emission model

Detailed process-based terrestrial ecosystem models that simulate biogeochemical cycles and vegetation are available (Bona et al., 2020; Oikawa et al., 2017; Wu and Blodau, 2013). Such modelling schemes rely largely on multiple parameters related to plant and soil biogeochemistry which are not generally attainable, thereby limiting the possibility to generalize and upscale.

As an alternative a range of empirical models with varying levels of complexity has been developed to describe ecosystem respiration; however, the most commonly applied formulation is the Lloyd–Taylor model (Lloyd J., Taylor, 1994), in which temperature acts as the sole independent variable. Structural complexity in empirical equations is increased through the integration of various other environmental variables, for example, hydrological variables such as WTD (Rigney et al., 2018). Recent alternative empirical approaches for estimating CO_2 emissions for organics soils include response functions linking average annual WTD to annual emissions (Arents et al., 2018; Evans et al., 2021; Tiemeyer et al., 2020), such as the *Annual WTD model* (Koch et al., 2023) used in this study.

To evaluate alternative empirical emission models alongside our *Daily WTD-T_{air} model,* we fitted three different empirical formulations from Rigney et al. (2018) to the Vejrumbro soil CO_2 flux data (Table S7). Each of the three empirical formulations incorporated both temperature and WTD as independent variable. The model fitting resulted in R^2 values comparable to those obtained from fitting the *Daily WTD-T_{air} model* developed in this study (Table S7).

Studying the explanatory power of each independent variable of WTD and T_{air} in isolation in the other empirical emission models, revealed that models in which WTD and T_{air} are incorporated as additive terms, rather than as interdependent (e.g., multiplicative) terms (as in eq. 6 and 8 in Rigney et al., (2018)), often exhibit coefficients of determination (R^2) that are excessively dominated by either WTD or T_{air} (Table S7). This indicates that such model formulations may inadequately capture the joint or synergistic effects of these variables on the dependent variable. The challenge likely stems from the fact that both WTD and T_{air} exhibit similar seasonal patterns, which may lead the regression to primarily fit one of the additive terms containing either WTD or T_{air}. Empirical models that incorporate WTD and T_{air} as multiplicative terms (such as equation 7 in Rigney et al. (2018) and the *Daily WTD-T_{air}* model developed in this study) demonstrate a more balanced distribution of explanatory power between each independent variable (Table S7). Nevertheless, equation [7] in Rigney et al. (2018) remains predominantly influenced by the T_{air} component (Table S7). A more balanced distribution of explanatory power between temperature and WTD is desirable, given that both variables are recognized as key drivers of soil CO_2 flux dynamics, which is achieved better with the *Daily WTD-T_{air}* than with any of the empirical models in Table S7.

We acknowledge that the *Daily WTD-T_{air} model* does not reproduce many of the highest observed fCO_2 values (Figure S6 and S7). In addition to identifying a relationship between fCO_2 and WTD, which was used to derive the *Daily WTD-T_{air} model* (Figure S5), we studied the temperature sensitivity within WTD bins to better understand the model's inability to reproduce the highest observed fCO_2 values. Specifically, we binned the daily fCO_2 into four WTD intervals: <20 cm (n=73), 20 to 40 cm (n=37), 30 to 40 cm (n=77) and >40 cm (n=44) (Figure S9). We identified a potential relationship between fCO_2 and temperature within WTD bins (Figure S9). This result is expected given the strong interdependence among fCO_2, temperature and WTD, all of which exhibit comparable seasonal dynamics. The high observed fCO_2 values cannot be captured by a simple empirical model based solely on T_{air} and WTD, particularly because both high and low fCO_2 occur under similar T_{air} and WTD conditions (Figure S5, S7 and S9). Consequently, the *Daily WTD-T_{air} model* represents a compromise that captures part of the variability while preserving a realistic mean response.

In this study, we demonstrate the need for the development of emission models operating on a sub-annual timescale. It highlights the necessity of creating scalable generalized models based on temperature, WTD and possibly other predictors. The development of such models requires data from a large number of sites with continuous and temporally dense measurement, in order to integrate information in a manner similar to models based on annual WTD. We recognize that currently, models based on annual WTD are likely the most robust for upscaling to national level and current conditions.

The simulated soil CO_2 flux at Vejrumbro, estimated using the *Daily WTD-T_{air}* model (13.6 Mg CO_2-C ha^{-1} yr^{-1}), aligns well with flux measurements from Danish and German sites (Figure 5). This agreement suggests a comparable magnitude of emissions across geographically distinct locations of similar characteristics, such as soil type and land use history.

We acknowledge that the *Daily WTD-T_{air} model* is derived from a single dataset, and that other emission models also provide valid fits of WTD and T_{air}. Furthermore, we recognize that empirical emission models are highly dependent on the specific data to which they are fitted. Acknowledging the limited data behind the *Daily WTD-T_{air} model* utilized in this study, the goal has not been to accurately estimate the peatland emission budget, which will be uncertain due to the reliance on a single site. However, the objective has been to illustrate the impact and insights gained from applying emission models at a daily timescale and how this has significant impact on the conclusions that can be made regarding effects of rewetting and climate change. The decision to utilize the *Daily WTD-T_{air} model* for rewetting and climate modeling scenarios is motivated by the simplicity of the relationship and its direct derivation from the Vejrumbro data, which clearly demonstrates a temperature-dependent relationship between soil CO_2 flux and WTD. The limited availability of multiple high-temporal-resolution GHG emission datasets broadly restricts the ability to generalize and upscale empirical GHG emission models at a daily timescale. Therefore, we consider the *Daily WTD-T_{air}* model to be the most reliable option currently available. Future research should validate the performance of emission models on intra-annual (within years) data with continuous measured CO_2 data.

A promising methodology for future applications, as well as for integrating a Tier 3 framework, involves coupling a process-based hydrological model with process-based emission models or an empirically derived daily emission model, such as the one developed in this study, to enable detailed simulations of GHG emissions that capture short-term dynamics and compound environmental effects.

Conclusion

This study demonstrates the feasibility of simulating the temporal dynamics of the peatland water balance and shallow groundwater table depth (WTD) using a catchment-scale distributed hydrological model. Accurately modelling shallow WTD is critical for reliable projections of CO_2 emissions from peatlands. We combined simulations of shallow WTD from the calibrated hydrological model with two empirical CO_2 emission models 1) an annual WTD-CO_2 relationship and 2) a daily WTD-CO_2 model accounting for the temperature effect on soil CO_2 production. This approach was used to estimate net soil CO_2 emissions for the historical period (1991-2020), the mid-century period (2041-2070) and the end-of-century period (2071-2100). This demonstrated that projections of soil CO_2 emissions are highly sensitive to the complexity and temporal resolution of the emission model applied. Specifically, models that incorporate both temperature and WTD dynamics at a daily timescale results in vastly different conclusion regarding impacts of climate change and rewetting. Regarding climate change impacts, we show that a daily temperature and WTD based emission model predict increased emissions due to temperature changes, which can be counter balanced (in the Danish case) or amplified depending on the future trend in WTD. Our results also demonstrate that rewetting strategies aimed at raising the groundwater table during the warm summer period offer a CO_2 emission reduction potential of up to 50%, whereas approaches focused primarily on increasing winter water table levels result in only marginal reductions. The combination of process-based hydrological model simulations and a daily-resolution empirical CO_2 emission model used in this study captures the influence of short-term compound climate events—such as simultaneous high temperatures and low WTD—which substantially alters projected emission trends compared to simpler approaches. Such refined approaches are essential for developing adaptive, climate-resilient peatland restoration policies and improving national greenhouse gas inventories. The findings underscore the importance of moving beyond static, annual WTD thresholds in peatland management by incorporating dynamic hydrological simulations. Instead, rewetting strategies should prioritize maintaining elevated summer groundwater table levels to buffer against drought-induced emission peaks.

Supplement link

…

Author contributions

All authors contributed to the conception and design of the study. TD conducted the analysis and drafted the manuscript, with input and revisions from all co-authors.

Competing interests

The authors declare that they have no conflict of interest.

Acknowledgements

We would like to thank Independent Research Fund Denmark for supporting the project PEAtlands and Climate-driven variability in groundwater depth – Impacts on greenhouse gas Emissions.

References

Adhikari, K., Hartemink, A. E., Minasny, B., Bou Kheir, R., Greve, M. B., and Greve, M. H.: Digital mapping of soil organic carbon contents and stocks in Denmark, PLoS One, 9, https://doi.org/10.1371/journal.pone.0105519, 2014.

Ala-aho, P., Soulsby, C., Wang, H., and Tetzlaff, D.: Integrated surface-subsurface model to investigate

the role of groundwater in headwater catchment runoff generation: A minimalist approach to parameterisation, J. Hydrol., 547, 664–677, https://doi.org/10.1016/j.jhydrol.2017.02.023, 2017.

Arents, E. J. M. M., van der Kolk, J. W. H., Hengeveld, G. M., Lesschen, J. P., Kramer, H., Kuikman, P. J., and Schelhaas, M. J.: Greenhouse gas reporting for the LULUCF sector in the Netherlands - Methodological background, updata 2018, Wageningen, WOt-technical report 113., 2018.

Asadzadeh, M. and Tolson, B.: Pareto archived dynamically dimensioned search with hypervolume-based selection for multi-objective optimization, Eng. Optim, 45, 1489–1509, https://doi.org/https://doi.org/10.1080/0305215X.2012.748046, 2013.

Autio, A., Aho, P. A., Ronkanen, A. K., Rossi, P. M., and Kløve, B.: Implications of Peat Soil Conceptualization for Groundwater Exfiltration in Numerical Modeling: A Study on a Hypothetical Peatland Hillslope, Water Resour. Res., https://doi.org/10.1029/2019WR026203, 2020.

Bechtold, M., Tiemeyer, B., Laggner, A., Leppelt, T., Frahm, E., and Belting, S.: Large-scale regionalization of water table depth in peatlands optimized for greenhouse gas emission upscaling, Hydrol. Earth Syst. Sci., 18, 3319–3339, https://doi.org/10.5194/hess-18-3319-2014, 2014.

Bechtold, M., Lannoy, G. J. M. De, Koster, R. D., Reichle, R. H., Mahanama, S. P., Bleuten, W., Bourgault, M. A., Brümmer, C., Burdun, I., Desai, A. R., Devito, K., Grünwald, T., Grygoruk, M., Humphreys, E. R., Klatt, J., Kurbatova, J., Lohila, A., Munir, T. M., Nilsson, M. B., Price, J. S., Röhl, M., Schneider, A., and Tiemeyer, B.: PEAT-CLSM: A Specific Treatment of Peatland Hydrology in the NASA Catchment Land Surface Model, J. Adv. Model. Earth Syst., 2130–2162, https://doi.org/10.1029/2018MS001574, 2019.

Bechtold, M., Lannoy, G. J. M. De, Reichle, R. H., Roose, D., Balliston, N., Burdun, I., Devito, K., Kurbatova, J., Strack, M., Zarov, E. A., States, U., Hydrology, W., Sciences, B., and Climate, G.: Improved Groundwater Table and L-band Brightness Temperature Estimates for Northern Hemisphere Peatlands Using New Model Physics and SMOS Observations in a Global Data Assimilation Framework, Remote Sens. Environ., 246, 2020.

Bleuten, W., Zarov, E., and Schmitz, O.: A high-resolution transient 3-dimensional hydrological model of an extensive undisturbed bog complex in West Siberia, Mires Peat, 26, 1–25, https://doi.org/10.19189/MaP.2019.OMB.StA.1769, 2020.

Bona, K. A., Shaw, C., Thompson, D. K., Hararuk, O., Webster, K., Zhang, G., Voicu, M., and Kurz, W. A.: The Canadian model for peatlands (CaMP): A peatland carbon model for national greenhouse gas reporting, Ecol. Modell., 431, 109164, https://doi.org/10.1016/j.ecolmodel.2020.109164, 2020.

Børgesen, C. D., Waagepetersen, J., Iversen, T. M., Grant, R., Jacobsen, B., and Elmhold, S.: Midtvejsevaluering af vandmiljøplan III - Hoved- og baggrundsnotater, 2009.

Bradley, C.: Simulation of the annual water table dynamics of a foodplain wetland, Narborough Bog , UK, J. Hydrol., 261, 150–172, 2002.

DHI: MIKE HYDRO - River - User Guide, Hørsholm, Denmark, 2019.

DHI: MIKE SHE - User Guide and Reference Manual, Hørsholm, Denmark, 2022.

Duranel, A., Thompson, J. R., Burningham, H., Durepaire, P., Garambois, S., Wyns, R., and Cubizolle, H.: Modelling the hydrological interactions between a fissured granite aquifer and a valley mire in the Massif Central, France, Hydrol. Earth Syst. Sci., 25, 291–319, 2021.

Evans, C. D., Peacock, M., Baird, A. J., Artz, R. R. E., Burden, A., Callaghan, N., Chapman, P. J., Cooper, H. M., Coyle, M., Craig, E., Cumming, A., Dixon, S., Gauci, V., Grayson, R. P., Helfter, C., Heppell, C. M., Holden, J., Jones, D. L., Kaduk, J., Levy, P., Matthews, R., McNamara, N. P., Misselbrook, T., Oakley, S., Page, S. E., Rayment, M., Ridley, L. M., Stanley, K. M., Williamson, J. L., Worrall, F., and Morrison, R.:

Overriding water table control on managed peatland greenhouse gas emissions, Nature, 593, 548–552, https://doi.org/10.1038/s41586-021-03523-1, 2021.

Friedrich, S., Gerner, A., Gabrielle, C., and Disse, M.: Scenario-based groundwater modeling of a raised bog with Mike She, EGU Gen. Assem. 2023, Vienna, Austria, 24–28 Apr 2023, EGU23-15608, https://doi.org/https://doi.org/10.5194/egusphere-egu23-15608, 2023.

Jupiter: https://www.geus.dk/produkter-ydelser-og-faciliteter/data-og-kort/national-boringsdatabase-jupiter, last access: 12 April 2025.

Graham, D. N. and Butts, M. B.: Flexible Integrated Watershed Modeling with MIKE SHE, in: Watershed Models, edited by: Singh, V. P. and Frevert, D. K., CRC Press, 245–272, https://doi.org/10.1201/9781420037432.ch10, 2005.

Günther, A., Barthelmes, A., Huth, V., Joosten, H., Jurasinski, G., Koebsch, F., and Couwenberg, J.: Prompt rewetting of drained peatlands reduces climate warming despite methane emissions, Nat. Commun., 11, 1–5, https://doi.org/10.1038/s41467-020-15499-z, 2020.

Gyldenkærne, S., Callisen, L. W., Greve, M. H., Beucher, A. M., Weber, P. L., Elsgaard, L., Lærke, P. E., Stisen, S., Koch, J., and Levin, G.: Opgørelse af CO2-emissioner fra organiske jorde, Aarhus Universitet, DCE – Nationalt Center for Miljø og Energi, Fagligt notat nr. 2025|01, 29pp pp., 2025.

Haahti, K., Warsta, L., Kokkoneen, T., Younis, B. B., and Koivusalo, H.: Distributed hydrological modeling with channel network flow of a forestry drained peatland site, Water Resour. Res., 246–263, https://doi.org/10.1002/2015WR018038.Received, 2015.

Henriksen, H. J., Kragh, S. J., Gotfredsen, J., Ondracek, M., M, van, T., Jakobsen, A., Schneider, R., Koch, J., Troldborg, L., Rasmussen, P., Pasten-Zapata, E., and Stisen, S.: Dokumentationsrapport vedr. modelleverancer til Hydrologisk Informations- og Prognosesystem, 2020.

Henriksen, H. J., Schneider, R., Koch, J., Ondracek, M., Troldborg, L., Seidenfaden, I. K., Kragh, S. J., Bøgh, E., and Stisen, S.: A New Digital Twin for Climate Change Adaptation, Water Management, and Disaster Risk Reduction (HIP Digital Twin), Water (Switzerland), 15, https://doi.org/10.3390/w15010025, 2023.

IPCC: 2013 Supplement to the 2006 IPCC Guidelines for National Greenhouse Gas Inventories : Wetlands, edited by: Hiraishi, T., Krug, T., Tanabe, K., Srivastava, N., Baasansuren, J., Fukuda, M.Troxler, T. G., Published: IPCC, Switzerland, Switzerland, 2014.

Jacob, D., Petersen, J., Eggert, B., Alias, A., Christensen, O. B., Bouwer, L. M., Braun, A., Colette, A., Déqué, M., Georgievski, G., Georgopoulou, E., Gobiet, A., Menut, L., Nikulin, G., Haensler, A., Hempelmann, N., Jones, C., Keuler, K., Kovats, S., Kröner, N., Kotlarski, S., Kriegsmann, A., Martin, E., van Meijgaard, E., Moseley, C., Pfeifer, S., Preuschmann, S., Radermacher, C., Radtke, K., Rechid, D., Rounsevell, M., Samuelsson, P., Somot, S., Soussana, J. F., Teichmann, C., Valentini, R., Vautard, R., Weber, B., and Yiou, P.: EURO-CORDEX: New high-resolution climate change projections for European impact research, Reg. Environ. Chang., 14, 563–578, https://doi.org/10.1007/s10113-013-0499-2, 2014.

Jaros, A., Rossi, P. M., Ronkanen, A., and Kløve, B.: Parameterisation of an integrated groundwater-surface water model for hydrological analysis of boreal aapa mire wetlands, J. Hydrol., 575, 175–191, https://doi.org/10.1016/j.jhydrol.2019.04.094, 2019.

Java, O., Kohv, M., and Lõhmus, A.: Performance of a bog hydrological system dynamics simulation model in an ecological restoration context: Soomaa case study, Estonia, Water (Switzerland), 13, https://doi.org/10.3390/w13162217, 2021.

Jutebring, E., Johansson, E., Sjöberg, Y., Huseby, R., and Laudon, H.: Groundwater-surface water

interactions across scales in a boreal landscape investigated using a numerical modelling approach, J. Hydrol., 560, 184–201, https://doi.org/10.1016/j.jhydrol.2018.03.011, 2018.

Kirpotin, S. N., Antoshkina, O. A., Berezin, A. E., Elshehawi, S., Feurdean, A., Lapshina, E. D., Pokrovsky, O. S., Peregon, A. M., Semenova, N. M., Tanneberger, F., Volkov, I. V, and Volkova, I. I.: Great Vasyugan Mire: How the world ' s largest peatland helps addressing the world ' s largest problems, Ambio, 50, 2038–2049, https://doi.org/10.1007/s13280-021-01520-2, 2021.

Koch, J., Elsgaard, L., Greve, M. H., Gyldenkærne, S., Hermansen, C., Levin, G., Wu, S., and Stisen, S.: Water-table-driven greenhouse gas emission estimates guide peatland restoration at national scale, Biogeosciences, 20, 2387–2403, https://doi.org/https://doi.org/10.5194/bg-20-2387-2023, 2023.

Lambert, C., Larocque, M., Gagné, S., and Garneau, M.: Aquifer-Peatland Hydrological Connectivity and Controlling Factors in Boreal Peatlands, Front. Earts Sci., 10, https://doi.org/10.3389/feart.2022.835817, 2022.

Largeron, C., Krinner, G., Ciais, P., and Brutel-Vuilmet, C.: Implementing northern peatlands in a global land surface model: Description and evaluation in the ORCHIDEE high-latitude version model (ORC-HL-PEAT), Geosci. Model Dev., 11, 3279–3297, https://doi.org/10.5194/gmd-11-3279-2018, 2018.

Leifeld, J., Wüst-Galley, C., and Page, S.: Intact and managed peatland soils as a source and sink of GHGs from 1850 to 2100, Nat. Clim. Chang., 9, 945–947, https://doi.org/10.1038/s41558-019-0615-5, 2019.

Lewis, C., Albertson, J., Zi, T., Xu, X., and Kiely, G.: How does afforestation affect the hydrology of a blanket peatland? A modelling study, Hydrol. Process., 3588, 3577–3588, https://doi.org/10.1002/hyp.9486, 2013.

Lloyd J., Taylor, J. A.: On the Temperature Dependence of Soil Respiration, Funct. Ecol., 8, 315–323, 1994.

Matott, L. S.: OSTRICH – An Optimization Software Toolkit for Research Involving Computational Heuristics Documentation and User ' s Guide, Version 17.12.19, New York, 2019.

Mozafari, B., Bruen, M., Donohue, S., Renou-wilson, F., and Loughlin, F. O.: Peatland dynamics: A review of process-based models and approaches Science of the Total Environment Peatland dynamics : A review of process-based models and approaches, Sci. Total Environ., 877, https://doi.org/10.1016/j.scitotenv.2023.162890, 2023.

Naturstyrelsen: Lavbundsprojekt Ringfenner, Detail- og Myndighedsprojekt, 2022.

Nielsen, A. S., Larsen, K. S., Lærke, P. L., Rodriguez, A. F., Pullens, J. W. M., Petersen, R. J., and Christiansen, J. R.: A full year of continuous net soil and ditch CO2, CH4, N2O fluxes, soil hydrology and meteorology for a drained fen in Denmark, Earth Syst. Sci. Data Discuss. [preprint], https://doi.org/10.5194/essd-2025-123, 2025a.

Nielsen, O.-K., Plejdrup, M. S., Winther, M., Nielsen, M., Gyldenkærne, S., Mikkelsen, M. H., Albrektsen, R., Hjelgaard, K., Fauser, P., Bruun, H. G., Levin, G., Callisen, L. W., Andersen, T. A., Johannsen, V. K., Nord-Larsen, T., Vesterdal, L., Stupak, I., Scott-Bentsen, N., Rasmussen, E., Petersen, S. B., Baunbæk, L., and Hansen, M. G.: Denmark's National Inventory Document 2025. Emission Inventories 1990-2023 - Submitted under the United Nations Framework Convention on Climate Change and the Paris Agreement, 2025b.

Oikawa, P. Y., Jenerette, G. D., Knox, S. H., Sturtevant, C., Verfaillie, J., Dronova, I., Poindexter, C. M., Eichelmann, E., and Baldocchi, D. D.: Evaluation of a hierarchy of models reveals importance of substrate limitation for predicting carbon dioxide and methane exchange in restored wetlands, J. Geophys. Res. Biogeosciences, 122, 145–167, https://doi.org/10.1002/2016JG003438, 2017.

997 Olefeldt, D., Euskirchen, E. S., Harden, J., Kane, E., McGuire, A. D., Waldrop, mark P., and Turetsky, M.
998 R.: A decade of boreal rich fen greenhouse gas fluxes in response to natural and experimental water
999 table variability, Glob. Chang. Biol., 23, 2428–2440, https://doi.org/10.1111/gcb.13612, 2017.

1000 Pasten-Zapata, E., Sonnenborg, T. O., and Refsgaard, J. C.: Climate change: Sources of uncertainty in
1001 precipitation and temperature projections for Denmark, Geol. Surv. Denmark Greenl. Bull., 43, 1–6,
1002 https://doi.org/10.34194/GEUSB-201943-01-02, 2019.

1003 Regeringen: Aftale om et Grønt Danmark - Aftale mellem regeringen, Landbrug & Fødevarer,
1004 Danmarks Naturfredningsforening, Fødevareforbundet NNF, Dansk Metal, Dansk Industri og
1005 Kommunernes Landsforening - 24. juni 2024, 2024.

1006 Regulation (EU) 2024/1991: of the European Parliament and of the Council of 24 June 2024 on nature
1007 restoration and amending Regulation (EU) 2022/869, Official Journal of the European Union, 2024.

1008 Rigney, C., Wilson, D., Renou-Wilson, F., Müller, C., Moser, G., and Byrne, K. A.: Greenhouse gas
1009 emissions from two rewetted peatlands previously managed for forestry, Mires Peat, 21, 1–23,
1010 https://doi.org/10.19189/MaP.2017.OMB.314, 2018.

1011 Rodriguez, A. F., Pullens, J. W. M., Christiansen, J. R., Larsen, K. S., and Lærke, P. E.: Modeling of
1012 greenhouse gas emissions from paludiculture in rewetting peatlands is improved by high frequency
1013 water table data, Egusph. [preprint], https://doi.org/10.5194/egusphere-2024-3030, 2024.

1014 Rossi, P. M., Ala-aho, P., and Doherty, J.: Impact of peatland drainage and restoration on esker
1015 groundwater resources: modeling future scenarios for management, Hydrogeol. J., 1131–1145,
1016 https://doi.org/10.1007/s10040-014-1127-z, 2014.

1017 Scharling, M.: Klimagrid Danmark - Nedbør, lufttemperatur og potentiel fordampning 20X20 & 40x40
1018 km - Metodebeskrivelse, Danish Meteorological Institute, 1999a.

1019 Scharling, M.: Klimagrid Danmark Nedbør 10x10 km (ver. 2) - Metodebeskrivelse, Danish
1020 Meteorological Institute, 1999b.

1021 Schneider, R., Koch, J., Troldborg, L., Henriksen, H. J., and Stisen, S.: Machine learning-based
1022 downscaling of modelled climate change impacts on groundwater table depth, 2022.

1023 Seidenfaden, I. K., Sonnenborg, T. O., Stisen, S., and Kidmose, J.: Quantification of climate change
1024 sensitivity of shallow and deep groundwater in Denmark, J. Hydrol. Reg. Stud., 41, 101100,
1025 https://doi.org/10.1016/j.ejrh.2022.101100, 2022.

1026 Shi, X., Thornton, P. E., Ricciuto, D. M., Hanson, P. J., Mao, J., Sebestyen, S. D., Griffiths, N. A., and
1027 Bisht, G.: Representing northern peatland microtopography and hydrology within the Community Land
1028 Model, Biogeosciences, 12, 6463–6477, https://doi.org/10.5194/bg-12-6463-2015, 2015.

1029 Stenberg, L., Haahti, K., Hökkä, H., Launiainen, S., and Nieminen, M.: Hydrology of Drained Peatland
1030 Forest: Numerical Experiment on the Role of Tree Stand Heterogeneity and Management, For. MDPI,
1031 1–19, https://doi.org/10.3390/f9100645, 2018.

1032 Stisen, S., Sonnenborg, T. O., Troldborg, L., and Refsgaard, J. C.: Evaluation of Climate Input Biases and
1033 Water Balance Issues Using a Coupled Surface – Subsurface Model, Vadose Zo. J., 10,
1034 https://doi.org/10.2136/vzj2010.0001, 2011.

1035 Stisen, S., Ondracek, M., Troldborg, L., Schneider, R. J. M., and van Til, M. J.: National Vandressource
1036 Model - Modelopstilling og kalibrering af DK-model 2019, De nationale geologiske undersøgelser for
1037 Danmark og Grønland (GEUS), Rapport 2019/31, 2019.

1038 Tanneberger, F., Abel, S., Couwenberg, J., Dahms, T., Gaudig, G., Günther, A., Kreyling, J., Peters, J.,
1039 Pongratz, J., and Joosten, H.: Towards net zero CO2 in 2050: An emission reduction pathway for

organic soils in germany, Mires Peat, 27, 1–17, https://doi.org/10.19189/MaP.2020.SNPG.StA.1951, 2021.

Thompson, C., Devito, K. J., and Mendoza, C. A.: Hydrologic impact of aspen harvesting within the subhumid Boreal Plains of Alberta, Hydrol. Process., 3924–3937, https://doi.org/10.1002/hyp.13301, 2018.

Tiemeyer, B., Freibauer, A., Borraz, E. A., Augustin, J., Bechtold, M., Beetz, S., Beyer, C., Ebli, M., Eickenscheidt, T., Fiedler, S., Förster, C., Gensior, A., Giebels, M., Glatzel, S., Heinichen, J., Hoffmann, M., Höper, H., Jurasinski, G., Laggner, A., Leiber-Sauheitl, K., Peichl-Brak, M., and Drösler, M.: A new methodology for organic soils in national greenhouse gas inventories: Data synthesis, derivation and application, Ecol. Indic., 109, 105838, https://doi.org/10.1016/j.ecolind.2019.105838, 2020.

Wilson, D., Blain, D., Couwenber, J., Evans, C., Murdiyarso, D., Page, S., Renou-Wilson, F., Rieley, J., Strack, M., and Tuittila, E. S.: Greenhouse gas emission factors associated with rewetting of organic soils, Mires Peat, 17, 1–28, https://doi.org/10.19189/MaP.2016.OMB.222, 2016.

Wu, Y. and Blodau, C.: PEATBOG: A biogeochemical model for analyzing coupled carbon and nitrogen dynamics in northern peatlands, Geosci. Model Dev., 6, 1173–1207, https://doi.org/10.5194/gmd-6-1173-2013, 2013.

Wunsch, A., Liesch, T., and Broda, S.: Deep learning shows declining groundwater levels in Germany until 2100 due to climate change, Nat. Commun., 13, 1–13, https://doi.org/10.1038/s41467-022-28770-2, 2022.

Yuan, F., Wang, Y., Ricciuto, D. M., Shi, X., Yuan, F., Brehme, T., Bridgham, S., Keller, J., Warren, J. M., Griffiths, N. A., Sebestyen, S. D., Hanson, P. J., Thornton, P. E., and Xu, X.: Hydrological feedbacks on peatland CH4 emission under warming and elevated CO2: A modeling study, J. Hydrol., 603, 127137, https://doi.org/10.1016/j.jhydrol.2021.127137, 2021.

Zscheischler, J., Martius, O., Westra, S., Bevacqua, E., Raymond, C., Horton, R. M., van den Hurk, B., AghaKouchak, A., Jézéquel, A., Mahecha, M. D., Maraun, D., Ramos, A. M., Ridder, N. N., Thiery, W., and Vignotto, E.: A typology of compound weather and climate events, Nat. Rev. Earth Environ., 1, 333–347, https://doi.org/10.1038/s43017-020-0060-z, 2020.